Toward NNLL threshold resummation for hadron pair production in hadronic collisions

Patriz Hinderer, Felix Ringer, George F. Sterman, and Werner Vogelsang

Phys. Rev. D **91**, 014016 — Published 14 January 2015

DOI: 10.1103/PhysRevD.91.014016

YITP-SB-14-44

Toward NNLL Threshold Resummation for Hadron Pair Production in Hadronic Collisions

Patriz Hinderer[a], **Felix Ringer**[a], **George F. Sterman**[b], **Werner Vogelsang**[a]

[a] Institute for Theoretical Physics, Tübingen University, Auf der Morgenstelle 14, 72076 Tübingen, Germany

[b] C.N. Yang Institute for Theoretical Physics, Stony Brook University, Stony Brook, New York 11794 – 3840, U.S.A.

Abstract

We investigate QCD threshold resummation effects beyond the next-to-leading logarithmic (NLL) order for the process $H_1H_2 \to h_1h_2X$ at high invariant mass of the produced hadron pair. We take into account the color structure of the underlying partonic hard-scattering cross sections and determine the relevant hard and soft matrices in color space that contribute to the resummed cross section at next-to-next-to-leading logarithmic (NNLL) accuracy. We present numerical results for fixed-target and collider regimes. We find a significant improvement compared to previous results at NLL accuracy. In particular, the scale dependence of the resummed cross section is greatly reduced. Use of the most recent set of fragmentation functions also helps in improving the comparison with the experimental data. Our calculation provides a step towards a systematic NNLL extension of threshold resummation also for other hadronic processes, in particular for jet production.

1 Introduction

The resummation of threshold logarithms in partonic hard-scattering cross sections contributing to hadronic scattering has received an ever-growing attention in recent years. On the one hand, resummation is phenomenologically relevant in many kinematical situations, ranging from fixed-target energies all the way to the LHC. At the same time, it offers insights into the structure of perturbative corrections at higher orders, which among other things may provide benchmarks for explicit full fixed-order calculations in QCD.

Threshold logarithms typically arise when the initial partons have just enough energy to produce the observed final state. In this case, the phase space available for gluon bremsstrahlung vanishes, resulting in large logarithmic corrections. Taking the hadron-pair production cross section to be discussed in this paper as an example, the partonic threshold is reached when $\hat{s} = \hat{m}^2$, that is, $\hat{\tau} \equiv \hat{m}^2/\hat{s} = 1$, where $\sqrt{\hat{s}}$ is the partonic center-of-mass system (c.m.s.) energy and $\hat{m}$ the pair mass of two outgoing produced partons that eventually fragment into the observed hadron pair. The leading large contributions near threshold arise as $\alpha_s^k \left[\ln^{2k-1}(1-\hat{\tau})/(1-\hat{\tau})\right]_+$ at the kth order in perturbation theory, where α_s is the strong coupling and the "plus" distribution will be defined below. There is a double-logarithmic structure, with two powers of the logarithm arising for every new order in the coupling. Subleading terms have fewer logarithms, so that the threshold logarithms in the perturbative series take the general form

$$\sum_{k=0}^{\infty} \sum_{\ell=1}^{2k} \alpha_s^k \, \mathcal{A}_{k,\ell} \left(\frac{\ln^{2k-\ell}(1-\hat{\tau})}{1-\hat{\tau}} \right)_+ , \tag{1}$$

with perturbative coefficients $\mathcal{A}_{k,\ell}$. One often refers to the all-order set of logarithms with a fixed ℓ as the ℓth *tower* of logarithms. As has been established in the literature [1, 2, 3], threshold logarithms exponentiate after taking an integral transform conjugate to the relevant kinematical variable ($\hat{\tau}$ in the above example). Under this transform the threshold logarithms translate into logarithms of the transform variable N. The exponent may itself be written as a perturbative series and is only *single-logarithmic* in the transform variable. Ignoring for the moment the color structure of the underlying partonic cross section, the structure of the resummed cross section becomes in transform space

$$\left(1 + \alpha_s C^{(1)} + \alpha_s^2 C^{(2)} + \ldots\right) \exp\left[\sum_{k=1}^{\infty} \sum_{\ell=1}^{k+1} \mathcal{B}_{k,\ell} \alpha_s^k \, \ln^{\ell}(N) \right] , \tag{2}$$

again with coefficients $\mathcal{B}_{k,\ell}$ and with "matching coefficients" $C^{(k)}$ that ensure that at every fixed order the resummed cross section agrees with the exact fixed-order one, up to corrections suppressed at threshold. They contain the full virtual corrections at order α_s^k, corresponding to contributions $\propto \delta(1-\hat{\tau})$ in the partonic cross section, and may be compared by comparison to a full fixed-order calculation performed near threshold. Thanks to the exponentiated single-logarithmic structure of the exponent, knowledge of the two leading towers $\alpha_s^k \ln^{k+1}(N)$ and $\alpha_s^k \ln^k(N)$, along with the coefficient $C^{(1)}$, is sufficient to predict the *three* leading towers in the perturbative series (1) for the cross section in $\hat{\tau}$-space. This is termed "next-to-leading logarithmic" (NLL) resummation. At full next-to-next-to-leading logarithmic (NNLL) accuracy, one needs three towers in the exponent and the two-loop coefficient $C^{(2)}$, providing control of already five towers in the partonic cross section.

While NLL resummation was the state of the art for many years, much progress has been made recently on extending the framework to NNLL accuracy, or even beyond. The most advanced results have been obtained for color-singlet processes such as Higgs production, where NNLL [4, 5] and, most recently, even studies up to the N^{3}LL level [6, 7] have been obtained, in which seven towers of logarithms are fully taken into account to all orders. This became possible when all threshold distributions at three-loop order were computed [8]. For processes that are not characterized by a color-singlet lowest-order (LO) hard scattering reaction, progress beyond NLL has also been made. For such processes, the resummation framework becomes more complex because the interference between soft emissions by the various external partons in the hard scattering process becomes sensitive to the color structure of the hard scattering itself. This requires a color basis for the partonic scattering process which, as will be reviewed below, leads to a matrix structure of the soft emission [2, 3, 9, 10]. This ultimately turns the exponential in (2) into a sum of exponentials, each with its own set of matching coefficients $C^{(k)}$. An extensive list of color-non-singlet reactions of this type along with corresponding references to NLL studies may be found in [11]. Resummation studies beyond NLL have been presented in the context of top quark pair production [12, 13], for single-inclusive hadron production [11], and for squark and gluino production [14]. At present, full NNLL resummation in the sense described above is not yet possible for most processes, since the required two-loop matching coefficients are usually not yet available (see, however, the recent calculation [15] for massless scattering). Nonetheless, already with knowledge of the one-loop matching coefficients an improvement of the resummation framework becomes possible, providing control of four (instead of five at full NNLL) towers in the partonic cross sections. A prerequisite for this is that the appropriate color structure be taken into account for all ingredients in the resummed expression.

In the present paper, we will develop such a partial NNLL resummation for the process of di-hadron production in hadronic collisions, collecting all necessary ingredients. Previously, Ref. [16] presented a NLL study for this process which forms the basis for our paper. Kinematically, hadron pair production shares many features with the much simpler color-singlet Drell-Yan process, if one confronts the produced partonic pair mass $\hat{m}$ with the invariant mass of the lepton pair. The interesting aspect of di-hadron production is that it possesses all the color complexity of the underlying $2 \to 2$ QCD hard scattering. As such, the process becomes an ideal test for the study of QCD resummation beyond NLL and can serve as a template for reactions of more significant phenomenological interest, especially single or two-jet production in hadronic collisions. That said, di-hadron production is phenomenologically relevant in its own right as experimental data as a function of the pair's mass are available from various fixed-target experiments [17, 18, 19], as well as from the ISR [20]. In addition, di-hadron cross sections are also accessible at the Relativistic Heavy Ion Collider (RHIC).

Our paper is structured as follows. In Sec. 2 we recall the basic formulas for the di-hadron cross section as a function of pair mass at fixed order in perturbation theory, and display the role of the threshold region. In order for this paper to be self-contained, we recall a number of results from [16]. Section 3 presents details of the NNLL threshold resummation for the cross section. In particular, we derive the various hard and soft matrices in color space that are needed for the analysis. Here, we make use of one-loop results available in the literature [21, 22, 23] and compare to related work [24]. In Sec. 4 we give phenomenological results, comparing the threshold resummed calculations at NLL and NNLL to some of the available experimental data. Finally, we summarize our results in Sec. 5.

2 Hadron pair production near partonic threshold

2.1 Perturbative cross section

As in [16], we consider the process $H_1(P_a) + H_2(P_b) \to h_1(P_c) + h_2(P_d) + X$ at measured pair invariant mass squared,

$$M^2 \equiv (P_c + P_d)^2 \,, \tag{3}$$

and at c.m.s. rapidities η_1, η_2 of the two produced hadrons. It is convenient to introduce

$$\begin{aligned} \Delta\eta &= \frac{1}{2}(\eta_1 - \eta_2) \,, \\ \bar{\eta} &= \frac{1}{2}(\eta_1 + \eta_2) \,. \end{aligned} \tag{4}$$

For sufficiently large M^2, the cross section for the process can be written in the factorized form

$$\begin{aligned} M^4 \frac{d\sigma^{H_1 H_2 \to h_1 h_2 X}}{dM^2 d\Delta\eta d\bar{\eta}} &= \sum_{abcd} \int_0^1 dx_a dx_b dz_c dz_d \, f_a^{H_1}(x_a,\mu_F) f_b^{H_2}(x_b,\mu_F) \, z_c D_c^{h_1}(z_c,\mu_F) z_d D_d^{h_2}(z_d,\mu_F) \\ &\quad \times \omega_{ab\to cd}\left(\hat{\tau}, \Delta\eta, \hat{\eta}, \alpha_s(\mu_R), \frac{\mu_R}{\hat{m}}, \frac{\mu_F}{\hat{m}}\right) \,, \end{aligned} \tag{5}$$

where $\hat{\eta}$ is the average rapidity in the partonic c.m.s., which is related to $\bar{\eta}$ by

$$\hat{\eta} = \bar{\eta} - \frac{1}{2}\ln\left(\frac{x_a}{x_b}\right) \,. \tag{6}$$

The quantity $\Delta\eta$ is a difference of rapidities and hence boost invariant. The average and relative rapidities for the hadrons and their parent partons are the same, since all particles are taken to be massless. The functions $f_{a,b}^{H_{1,2}}$ in Eq. (5) are the parton distribution functions for partons a, b in hadrons $H_{1,2}$ and $D_{c,d}^{h_{1,2}}$ the fragmentation functions for partons c, d fragmenting into the observed hadrons $h_{1,2}$. The distribution functions are evaluated at a factorization scale μ_F that we choose to be the same for the initial and the final state. μ_R denotes the renormalization scale, which may differ from μ_F. The partonic momenta are given in terms of the hadronic ones by $p_a = x_a P_a$, $p_b = x_b P_b$, $p_c = P_c/z_c$, $p_d = P_d/z_d$. We introduce

$$\begin{aligned} S &= (P_a + P_b)^2 \,, \\ \tau &\equiv \frac{M^2}{S} \,, \\ \hat{s} &\equiv (x_a P_a + x_b P_a)^2 = x_a x_b S \,, \\ \hat{m}^2 &\equiv \left(\frac{P_c}{z_c} + \frac{P_d}{z_d}\right)^2 = \frac{M^2}{z_c z_d} \,, \\ \hat{\tau} &\equiv \frac{\hat{m}^2}{\hat{s}} = \frac{M^2}{x_a x_b z_c z_d S} = \frac{\tau}{x_a x_b z_c z_d} \,. \end{aligned} \tag{7}$$

The $\omega_{ab\to cd}$ in Eq. (5) are the hard-scattering functions for the contributing partonic processes $ab \to cdX'$, where X' denotes some additional unobserved partonic final state. Since the cross

section in Eq. (5) has been written in a dimensionless form, the $\omega_{ab\to cd}$ can be chosen to be functions of $\hat{m}^2/\hat{s} = \hat{\tau}$ and the ratios of $\hat{m}$ to the factorization and renormalization scales, as well as the rapidities and the strong coupling. They may be computed in QCD perturbation theory, where they are expanded as

$$\omega_{ab\to cd} = \left(\frac{\alpha_s}{\pi}\right)^2 \left[\omega^{\rm LO}_{ab\to cd} + \frac{\alpha_s}{\pi}\,\omega^{\rm NLO}_{ab\to cd} + \left(\frac{\alpha_s}{\pi}\right)^2 \omega^{\rm NNLO}_{ab\to cd} + \dots\right] . \tag{8}$$

Here we have separated the overall power of $\mathcal{O}(\alpha_s^2)$, which arises because the leading order partonic hard-scattering processes are the ordinary $2 \to 2$ QCD scatterings.

2.2 Threshold limit

The limit $\hat{\tau} \to 1$ corresponds to the partonic threshold, where the hard-scattering uses all available energy to produce the pair. This is kinematically similar to the Drell-Yan process, if one thinks of the hadron pair replaced by a lepton pair. The presence of fragmentation of course complicates the analysis somewhat, because only a fraction $z_c z_d$ of $\hat{m}^2$ is used for the invariant mass of the observed hadron pair. As shown in [16], it is useful to introduce the variable

$$\tau' \equiv \frac{\hat{m}^2}{S} = \frac{M^2}{z_c z_d S} , \tag{9}$$

which may be viewed as the "τ-variable" at the level of produced partons when fragmentation has not yet been taken into account, akin to the variable $\tau = Q^2/S$ in Drell-Yan.

At LO, one has $\hat{\tau} = 1$ and also $\hat{\eta} = 0$. One can therefore write the LO term as

$$\omega^{\rm LO}_{ab\to cd}\,(\hat{\tau}, \Delta\eta, \hat{\eta}) = \delta\,(1-\hat{\tau})\;\delta\,(\hat{\eta})\;\omega^{(0)}_{ab\to cd}(\Delta\eta) , \tag{10}$$

where $\omega^{(0)}_{ab\to cd}$ is a function of $\Delta\eta$ only. According to (6), the second delta-function implies that $\bar{\eta} = \frac{1}{2}\ln(x_a/x_b)$. At next-to-leading order (NLO), or overall $\mathcal{O}(\alpha_s^3)$, one can have $\hat{\tau} \neq 1$ and $\hat{\eta} \neq 0$. In general, as discussed in [16], near partonic threshold the kinematics becomes "LO like". One has:

$$\begin{aligned}\omega_{ab\to cd}\left(\hat{\tau}, \Delta\eta, \hat{\eta}, \alpha_s(\mu_R), \frac{\mu_R}{\hat{m}}, \frac{\mu_F}{\hat{m}}\right) &= \delta\,(\hat{\eta})\;\omega^{\rm sing}_{ab\to cd}\left(\hat{\tau}, \Delta\eta, \alpha_s(\mu_R), \frac{\mu_R}{\hat{m}}, \frac{\mu_F}{\hat{m}}\right) \\ &+ \omega^{\rm reg}_{ab\to cd}\left(\hat{\tau}, \Delta\eta, \hat{\eta}, \alpha_s(\mu_R), \frac{\mu_R}{\hat{m}}, \frac{\mu_F}{\hat{m}}\right) ,\end{aligned} \tag{11}$$

where all singular behavior near threshold is contained in the functions $\omega^{\rm sing}_{ab\to cd}$. Threshold resummation addresses this singular part to all orders in the strong coupling. All remaining contributions, which are subleading near threshold, are collected in the "regular" functions $\omega^{\rm reg}_{ab\to cd}$. Specifically, for the NLO corrections, one finds the following structure:

$$\begin{aligned}\omega^{\rm NLO}_{ab\to cd}\left(\hat{\tau}, \Delta\eta, \hat{\eta}, \frac{\mu_R}{\hat{m}}, \frac{\mu_F}{\hat{m}}\right) &= \delta\,(\hat{\eta})\,\left[\omega^{(1,0)}_{ab\to cd}\left(\Delta\eta, \frac{\mu_R}{\hat{m}}, \frac{\mu_F}{\hat{m}}\right)\,\delta(1-\hat{\tau})\right. \\ &+ \omega^{(1,1)}_{ab\to cd}\left(\Delta\eta, \frac{\mu_F}{\hat{m}}\right)\left(\frac{1}{1-\hat{\tau}}\right)_+ + \left.\omega^{(1,2)}_{ab\to cd}(\Delta\eta)\left(\frac{\log(1-\hat{\tau})}{1-\hat{\tau}}\right)_+\right] \\ &+ \omega^{\rm reg,NLO}_{ab\to cd}\left(\hat{\tau}, \Delta\eta, \hat{\eta}, \frac{\mu_R}{\hat{m}}, \frac{\mu_F}{\hat{m}}\right) ,\end{aligned} \tag{12}$$

where the singular part near threshold is represented by the functions $\omega^{(1,0)}_{ab\to cd}, \omega^{(1,1)}_{ab\to cd}, \omega^{(1,2)}_{ab\to cd}$, which are again functions of only $\Delta\eta$, up to scale dependence. The "plus"-distributions are defined by

$$\int_{x_0}^1 f(x)\,(g(x))_+\,dx \equiv \int_{x_0}^1 (f(x)-f(1))\;g(x)dx - f(1)\int_0^{x_0} g(x)dx\;. \tag{13}$$

The functions $\omega^{(1,0)}_{ab\to cd}, \omega^{(1,1)}_{ab\to cd}, \omega^{(1,2)}_{ab\to cd}$ were derived in [16] from an explicit NLO calculation near threshold. We will use these results below as a useful check on the resummed formula and on the matching coefficients.

2.3 Mellin and Fourier transforms

In order to prepare the resummation of threshold logarithms, we take integral transforms of the cross section. Following [16], we first write the hadronic cross section in Eq. (5) as

$$M^4\frac{d\sigma^{H_1H_2\to h_1h_2X}}{dM^2 d\Delta\eta d\bar\eta} = \sum_{cd}\int_0^1 dz_c\,dz_d\,z_c\,D_c^{h_1}(z_c,\mu_F)\,z_d\,D_d^{h_2}(z_d,\mu_F)\,\Omega_{H_1H_2\to cd}\left(\tau',\Delta\eta,\bar\eta,\alpha_s(\mu_R),\frac{\mu_R}{\hat m},\frac{\mu_F}{\hat m}\right), \tag{14}$$

where $\tau' = \hat m^2/S = \hat\tau x_a x_b$ and

$$\begin{aligned}\Omega_{H_1H_2\to cd}\left(\tau',\Delta\eta,\bar\eta,\alpha_s(\mu_R),\frac{\mu_R}{\hat m},\frac{\mu_F}{\hat m}\right) \;&\equiv\; \sum_{ab}\int_0^1 dx_a\,dx_b\,f_a^{H_1}(x_a,\mu_F)\;f_b^{H_2}(x_b,\mu_F)\\ &\quad\times\;\omega_{ab\to cd}\left(\hat\tau,\Delta\eta,\hat\eta,\alpha_s(\mu_R),\frac{\mu_R}{\hat m},\frac{\mu_F}{\hat m}\right).\end{aligned} \tag{15}$$

Taking Mellin moments of this function with respect to τ' and a Fourier transform in $\bar\eta$, we obtain

$$\begin{aligned}&\int_{-\infty}^{\infty} d\bar\eta\,e^{i\nu\bar\eta}\int_0^1 d\tau'\;(\tau')^{N-1}\,\Omega_{H_1H_2\to cd}\left(\tau',\Delta\eta,\bar\eta,\alpha_s(\mu_R),\frac{\mu_R}{\hat m},\frac{\mu_F}{\hat m}\right)\\ &\quad=\sum_{ab}\tilde f_a^{H_1}(N+1+i\nu/2,\mu_F)\tilde f_b^{H_2}(N+1-i\nu/2,\mu_F)\;\tilde\omega_{ab\to cd}\left(N,\nu,\Delta\eta,\alpha_s(\mu_R),\frac{\mu_R}{\hat m},\frac{\mu_F}{\hat m}\right),\end{aligned} \tag{16}$$

where $\tilde f_a^H(N,\mu_F)\equiv\int_0^1 x^{N-1}f_a^H(x,\mu_F)dx$, and

$$\tilde\omega_{ab\to cd}\left(N,\nu,\Delta\eta,\alpha_s(\mu_R),\frac{\mu_R}{\hat m},\frac{\mu_F}{\hat m}\right)\equiv\int_{-\infty}^{\infty}d\hat\eta\,e^{i\nu\hat\eta}\int_0^1 d\hat\tau\,\hat\tau^{N-1}\,\omega_{ab\to cd}\left(\hat\tau,\Delta\eta,\hat\eta,\alpha_s(\mu_R),\frac{\mu_R}{\hat m},\frac{\mu_F}{\hat m}\right). \tag{17}$$

Near threshold, keeping only the singular terms in (11), the right-hand-side of this reduces to

$$\int_0^1 d\hat\tau\,\hat\tau^{N-1}\,\omega^{\rm sing}_{ab\to cd}\left(\hat\tau,\Delta\eta,\alpha_s(\mu_R),\frac{\mu_R}{\hat m},\frac{\mu_F}{\hat m}\right)\;\equiv\;\tilde\omega^{\rm resum}_{ab\to cd}\left(N,\Delta\eta,\alpha_s(\mu_R),\frac{\mu_R}{\hat m},\frac{\mu_F}{\hat m}\right). \tag{18}$$

We have labeled the new function on the right by the superscript "resum" as it is this quantity that contains all threshold logarithms and that threshold resummation addresses. As discussed in [16], it is important here that we consider fixed $\hat m$ and fixed renormalization/factorization scales, which is achieved by isolating the fragmentation functions as in Eq. (14). Note that $\tilde\omega^{\rm resum}_{ab\to cd}$ depends on the Mellin variable N only. All dependence on the Fourier variable ν resides in the moments of the parton distribution functions.

3 Threshold resummation for hadron-pair production

In this section we present the framework for threshold resummation for di-hadron production at NNLL. We start by giving the main result and discussing its structure. Subsequently, we will describe the various new ingredients in more detail.

3.1 Resummation formula at next-to-next-to-leading logarithm

For di-hadron production near threshold, all gluon radiation is soft. Since all four external partons in the hard scattering are "observed" in the sense that they are either incoming or fragmenting partons, each of them makes the same type of (double-logarithmic) contribution to the resummed cross section in moment space, given by a "jet" function Δ_i^N $(i = a, b, c, d)$ that takes into account soft and collinear gluon radiation off an external parton [16, 25, 26]. In addition, large-angle soft emission is sensitive to the color state of the hard scattering, giving rise to a trace structure in color space [2, 9]. The resummed partonic cross section in moment space then takes the following form [2, 3, 9, 10, 16]:

$$\begin{aligned}
\tilde{\omega}_{ab\to cd}^{\rm resum}\left(N,\Delta\eta,\alpha_s(\mu_R),\frac{\mu_R}{\hat{m}},\frac{\mu_F}{\hat{m}}\right) &= \Delta_a^{N+1}\left(\alpha_s(\mu_R),\frac{\mu_R}{\hat{m}},\frac{\mu_F}{\hat{m}}\right)\Delta_b^{N+1}\left(\alpha_s(\mu_R),\frac{\mu_R}{\hat{m}},\frac{\mu_F}{\hat{m}}\right)\\
&\times\ \Delta_c^{N+2}\left(\alpha_s(\mu_R),\frac{\mu_R}{\hat{m}},\frac{\mu_F}{\hat{m}}\right)\Delta_d^{N+2}\left(\alpha_s(\mu_R),\frac{\mu_R}{\hat{m}},\frac{\mu_F}{\hat{m}}\right)\\
&\times\ {\rm Tr}\left\{H\left(\Delta\eta,\alpha_s(\mu_R)\right)\mathcal{S}_N^\dagger\left(\Delta\eta,\alpha_s(\mu_R),\frac{\mu_R}{\hat{m}}\right)\right.\\
&\qquad\left. S\left(\alpha_s(\hat{m}/\bar{N}),\Delta\eta\right)\mathcal{S}_N\left(\Delta\eta,\alpha_s(\mu_R),\frac{\mu_R}{\hat{m}}\right)\right\}_{ab\to cd}\\
&\times\ \xi_R\left(\alpha_s(\mu_R),\frac{\mu_R}{\hat{m}}\right)\xi_F^{abcd}\left(\alpha_s(\mu_R),\frac{\mu_F}{\hat{m}}\right)\ . \qquad (19)
\end{aligned}$$

This form is valid to all logarithmic order, up to corrections that are suppressed by powers of $1/N$, or $1-\hat{\tau}$. The additional functions $\xi_{R,F}$ do not contain threshold logarithms but are N-independent. They serve to improve the dependence of the resummed cross section on the scales μ_R and μ_F. We will now discuss the various functions in Eq. (19) and their NNLL expansions.

3.1.1 Jet functions

The radiative functions Δ_i^N are familiar from threshold resummation for the Drell-Yan process. They exponentiate logarithms that arise due to soft-collinear gluon emission by the initial and final-state partons. In the $\overline{\rm MS}$ scheme, they are given by [1, 4, 27]

$$\begin{aligned}
\Delta_i^N\left(\alpha_s(\mu_R),\frac{\mu_R}{\hat{m}},\frac{\mu_F}{\hat{m}}\right) &= R_i(\alpha_s(\mu_R))\,\exp\left\{\int_0^1\frac{z^{N-1}-1}{1-z}\right.\\
&\left.\times\left[\int_{\mu_F^2}^{(1-z)^2\hat{m}^2}\frac{d\mu^2}{\mu^2}A_i(\alpha_s(\mu))+D_i(\alpha_s((1-z)\hat{m}))\right]\right\}. \qquad (20)
\end{aligned}$$

The functions A_i and D_i may be calculated perturbatively as series in α_s,

$$\begin{aligned} A_i(\alpha_s) &= \frac{\alpha_s}{\pi} A_i^{(1)} + \left(\frac{\alpha_s}{\pi}\right)^2 A_i^{(2)} + \left(\frac{\alpha_s}{\pi}\right)^3 A_i^{(3)} + \mathcal{O}(\alpha_s^4) \\ D_i(\alpha_s) &= \left(\frac{\alpha_s}{\pi}\right)^2 D_i^{(2)} + \mathcal{O}(\alpha_s^3) \,, \end{aligned} \tag{21}$$

where, up to NNLL, one needs the coefficients [28, 29, 30, 31, 32]

$$\begin{aligned} A_i^{(1)} &= C_i \,, \qquad A_i^{(2)} = \frac{1}{2}\, C_i \left[C_A \left(\frac{67}{18} - \frac{\pi^2}{6} \right) - \frac{5}{9} N_f \right] \,, \\ A_i^{(3)} &= \frac{1}{4} C_i \left[C_A^2 \left(\frac{245}{24} - \frac{67}{9}\zeta(2) + \frac{11}{6}\zeta(3) + \frac{11}{5}\zeta(2)^2 \right) + C_F N_f \left(-\frac{55}{24} + 2\zeta(3) \right) \right. \\ &\qquad \left. + C_A N_f \left(-\frac{209}{108} + \frac{10}{9}\zeta(2) - \frac{7}{3}\zeta(3) \right) - \frac{1}{27} N_f^2 \right] \,, \\ D_i^{(2)} &= C_i \left[C_A \left(-\frac{101}{27} + \frac{11}{3}\zeta(2) + \frac{7}{2}\zeta(3) \right) + N_f \left(\frac{14}{27} - \frac{2}{3}\zeta(2) \right) \right] \,, \end{aligned} \tag{22}$$

with N_f the number of flavors and

$$C_q = C_F = \frac{N_c^2 - 1}{2N_c} = \frac{4}{3} \,, \quad C_g = C_A = N_c = 3 \,. \tag{23}$$

The D_i term in the radiative factor Δ_i^N first appears at NNLL accuracy [1, 4, 27]. It takes into account logarithms that arise from soft gluons that are emitted at large angles. Incoming and outgoing external lines of a given parton type carry the same D_i term, as discussed in the Appendix.

Finally, the coefficient R_i in Eq. (20) ensures that our soft functions for this process are defined relative to that for the Drell-Yan process; again see the Appendix for details. To the order we consider, we have

$$R_i(\alpha_s) \,=\, 1 - \frac{3\alpha_s}{4\pi}\, A_i^{(1)}\, \zeta(2) + \mathcal{O}(\alpha_s^2) \,. \tag{24}$$

Evaluating the integrals in Eq. (20), one obtains an explicit expression for the NNLL expansion of the function Δ_i^N:

$$\begin{aligned} \Delta_i^N \left(\alpha_s(\mu_R), \frac{\mu_R}{\hat{m}}, \frac{\mu_F}{\hat{m}} \right) &= \tilde{R}_i(\alpha_s(\mu_R)) \, \exp\left\{ h_i^{(1)}(\lambda)\, \ln \bar{N} + h_i^{(2)} \left(\lambda, \alpha_s(\mu_R), \frac{\mu_R}{\hat{m}}, \frac{\mu_F}{\hat{m}} \right) \right. \\ &\qquad \left. +\, \alpha_s(\mu_R)\, h_i^{(3)} \left(\lambda, \alpha_s(\mu_R), \frac{\mu_R}{\hat{m}}, \frac{\mu_F}{\hat{m}} \right) \right\} \,. \end{aligned} \tag{25}$$

Here $\tilde{R}_i$ is a combination of R_i in Eq. (24) and a π^2-term arising in the NNLL expansion [4]:

$$\tilde{R}_i(\alpha_s) \,=\, 1 + \frac{\alpha_s}{4\pi}\, A_i^{(1)}\, \zeta(2) + \mathcal{O}(\alpha_s^2) \,. \tag{26}$$

In (25) we have furthermore defined $\lambda = b_0 \alpha_s(\mu_R) \ln(N \mathrm{e}^{\gamma_E})$ with γ_E the Euler constant. In the

following we denote $N\mathrm{e}^{\gamma_E} \equiv \bar{N}$. The functions $h_i^{(1)}, h_i^{(2)}, h_i^{(3)}$ read

$$h_i^{(1)}(\lambda) = \frac{A_i^{(1)}}{2\pi b_0 \lambda} \left(2\lambda + (1-2\lambda)\ln(1-2\lambda)\right) , \tag{27}$$

$$\begin{aligned} h_i^{(2)}\left(\lambda, \alpha_s(\mu_R), \frac{\mu_R}{\hat{m}}, \frac{\mu_F}{\hat{m}}\right) &= -\frac{A_i^{(2)}}{2\pi^2 b_0^2}\left[2\lambda + \ln(1-2\lambda)\right] \\ &+ \frac{A_q^{(1)} b_1}{2\pi b_0^3}\left[2\lambda + \ln(1-2\lambda) + \frac{1}{2}\ln^2(1-2\lambda)\right] \\ &- \frac{A_i^{(1)}}{2\pi b_0}\left[2\lambda + \ln(1-2\lambda)\right]\ln\frac{\mu_R^2}{\hat{m}^2} + \frac{A_i^{(1)}}{\pi b_0}\lambda \ln\frac{\mu_F^2}{\hat{m}^2} , \end{aligned} \tag{28}$$

and [27]

$$\begin{aligned} h_i^{(3)}\left(\lambda, \alpha_s(\mu_R), \frac{\mu_R}{\hat{m}}, \frac{\mu_F}{\hat{m}}\right) &= \frac{2A_i^{(1)}}{\pi}\zeta(2)\frac{\lambda}{1-2\lambda} - \frac{A_i^{(2)} b_1}{2\pi^2 b_0^3}\frac{1}{1-2\lambda}\left[2\lambda + \ln(1-2\lambda) + 2\lambda^2\right] \\ &+ \frac{A_i^{(1)} b_1^2}{2\pi b_0^4 (1-2\lambda)}\left[2\lambda^2 + 2\lambda\ln(1-2\lambda) + \frac{1}{2}\ln^2(1-2\lambda)\right] \\ &+ \frac{A_i^{(1)} b_2}{2\pi b_0^3}\left[2\lambda + \ln(1-2\lambda) + \frac{2\lambda^2}{1-2\lambda}\right] + \frac{A_i^{(3)}}{\pi^3 b_0^2}\frac{\lambda^2}{1-2\lambda} \\ &+ \frac{A_i^{(2)}}{\pi^2 b_0}\lambda\ln\frac{\mu_F^2}{\hat{m}^2} - \frac{A_i^{(1)}}{2\pi}\lambda\ln^2\frac{\mu_F^2}{\hat{m}^2} + \frac{A_i^{(1)}}{\pi}\lambda\ln\frac{\mu_R^2}{\hat{m}^2}\ln\frac{\mu_F^2}{\hat{m}^2} \\ &- \frac{1}{1-2\lambda}\left(\frac{A_i^{(1)} b_1}{2\pi b_0^2}\left[2\lambda + \ln(1-2\lambda)\right] - \frac{2A_i^{(2)}}{\pi^2 b_0}\lambda^2\right)\ln\frac{\mu_R^2}{\hat{m}^2} \\ &+ \frac{A_i^{(1)}}{\pi}\frac{\lambda^2}{1-2\lambda}\ln^2\frac{\mu_R^2}{\hat{m}^2} - \frac{D_i^{(2)}}{2\pi^2 b_0}\frac{\lambda}{1-2\lambda} . \end{aligned} \tag{29}$$

Here b_0, b_1, b_2 are the first three coefficients of the QCD beta function which are given by [33, 34]

$$\begin{aligned} b_0 &= \frac{1}{12\pi}\left(11C_A - 2N_f\right) , \qquad b_1 = \frac{1}{24\pi^2}\left(17C_A^2 - 5C_A N_f - 3C_F N_f\right) , \\ b_2 &= \frac{1}{64\pi^3}\left(\frac{2857}{54}C_A^3 - \frac{1415}{54}C_A^2 N_f - \frac{205}{18}C_A C_F N_f + \frac{78}{54}C_A N_f^2 + \frac{11}{9}C_F N_f^2\right) . \end{aligned} \tag{30}$$

3.1.2 Color trace contribution

Next we discuss the trace $\mathrm{Tr}\{H\mathcal{S}_N^\dagger S\mathcal{S}_N\}$ in color space in Eq. (19). We note that this is the only contribution to the resummed cross section that depends on the difference of the rapidities $\Delta\eta$. Each of the functions $H_{ab\to cd}$, $\mathcal{S}_{N,ab\to cd}$, $S_{ab\to cd}$ is a matrix in the space of color exchange operators [2, 9]. The $H_{ab\to cd}$ are the hard-scattering functions. They are perturbative and have the expansions

$$H_{ab\to cd}\left(\Delta\eta, \alpha_s\right) = \left(\frac{\alpha_s}{\pi}\right)^2\left[H_{ab\to cd}^{(0)}\left(\Delta\eta\right) + \frac{\alpha_s}{\pi}H_{ab\to cd}^{(1)}\left(\Delta\eta\right) + \mathcal{O}(\alpha_s^2)\right] . \tag{31}$$

The LO (i.e. $\mathcal{O}(\alpha_s^2)$) contributions $H^{(0)}_{ab\to cd}$ may be found in [2, 9, 10]. For resummation beyond NLL accuracy, one needs all entries of the NLO hard-scattering matrices $H^{(1)}_{ab\to cd}$. These matrices may be extracted from a color decomposed one-loop calculation [16, 24]. We will outline the derivation of the first-order corrections $H^{(1)}_{ab\to cd}$ in Section 3.2. We note that they depend in principle also on the renormalization scale μ_R, in the form of a term $\propto \ln(\mu_R/\hat{m})H^{(0)}_{ab\to cd}$. This dependence, however, has been absorbed into the contribution involving the function ξ_R in (19); see below.

The $S_{ab\to cd}$ are known as soft functions. In general, they depend on the rapidity difference $\Delta\eta$ and on the strong coupling whose argument is to be set to $\hat{m}/\bar{N}$ [2, 9, 12]. This dependence on $\hat{m}/\bar{N}$ and hence on N occurs first at NNLL. The soft functions have the expansion

$$S_{ab\to cd}\left(\alpha_s(\hat{m}/\bar{N}),\Delta\eta\right) = S^{(0)}_{ab\to cd} + \frac{\alpha_s(\hat{m}/\bar{N})}{\pi} S^{(1)}_{ab\to cd}\left(\Delta\eta\right) + \mathcal{O}(\alpha_s^2)\ . \tag{32}$$

Relating the coupling at scale $\hat{m}/\bar{N}$ to that at scale μ_R, one can construct the explicit N-dependence of the soft matrix at NLO. To the accuracy of resummation that we are considering in this work, it is sufficient to use

$$\alpha_s(\hat{m}/\bar{N}) = \frac{\alpha_s(\mu_R)}{1-2\lambda}\ . \tag{33}$$

The LO expressions $S^{(0)}_{ab\to cd}$, which are independent of $\Delta\eta$, may also be found in [2, 9, 10]. Like the hard-scattering matrices $H^{(1)}_{ab\to cd}$, at NNLL accuracy, we need the explicit expressions for the full NLO soft-matrices $S^{(1)}_{ab\to cd}$. These may be extracted by performing a color-decomposed calculation of the $2\to 3$ contributions to the partonic cross sections in the eikonal approximation, as will be described in Section 3.3.

The resummation of wide-angle soft gluons is contained in $\mathcal{S}_{ab\to cd}$. The two exponentials $\mathcal{S}^\dagger_N$ and $\mathcal{S}_N$ that enclose the soft function $S_{ab\to cd}$ within the trace structure appear when solving the renormalization group equation for the soft function [2, 9, 10]. The exponentials are given in terms of soft anomalous dimensions $\Gamma_{ab\to cd}$:

$$\mathcal{S}_{N,ab\to cd}\left(\Delta\eta,\alpha_s(\mu_R),\frac{\mu_R}{\hat{m}}\right) \;=\; \mathcal{P}\exp\left[\frac{1}{2}\int_{\hat{m}^2}^{\hat{m}^2/\bar{N}^2}\frac{d\mu^2}{\mu^2}\Gamma_{ab\to cd}\left(\Delta\eta,\alpha_s(\mu)\right)\right]\ , \tag{34}$$

where $\mathcal{P}$ denotes path ordering. The soft anomalous dimension matrices start at $\mathcal{O}(\alpha_s)$,

$$\Gamma_{ab\to cd}\left(\alpha_s,\Delta\eta\right) = \frac{\alpha_s}{\pi}\,\Gamma^{(1)}_{ab\to cd}\left(\Delta\eta\right) + \left(\frac{\alpha_s}{\pi}\right)^2\,\Gamma^{(2)}_{ab\to cd}(\Delta\eta) + \mathcal{O}(\alpha_s^3)\ . \tag{35}$$

Their first-order terms are presented in [2, 9, 10, 35]. We will discuss the $\Gamma_{ab\to cd}$ matrices in more detail in Section 3.3. For NNLL resummation, we also need to take into account the second-order contributions $\Gamma^{(2)}_{ab\to cd}$ which were derived in [36] and are determined by the one-loop terms:

$$\Gamma^{(2)}_{ab\to cd}(\Delta\eta) = \frac{K}{2}\Gamma^{(1)}_{ab\to cd}(\Delta\eta)\ , \tag{36}$$

where $K = C_A(67/18-\pi^2/6)-5N_f/9$. We also give here our result for the NNLL expansion of

the integral in Eq. (34):

$$\ln \mathcal{S}_{N,ab\to cd}\left(\Delta\eta,\alpha_s,\frac{\mu_R}{\hat{m}}\right) = \Gamma^{(1)}_{ab\to cd}(\Delta\eta)\left[\frac{\ln(1-2\lambda)}{2\pi b_0}+\frac{\alpha_s}{\pi}\frac{1}{2b_0^2\pi(1-2\lambda)}\right.$$
$$\left.\times \left(b_1\pi(2\lambda+\ln(1-2\lambda)) - b_0\lambda\left(K+2\pi b_0\ln\frac{\mu_R^2}{\hat{m}^2}\right)\right)\right] . \quad (37)$$

We note that in our phenomenological applications we follow [16] and perform the exponentiation of the matrices numerically by iterating the exponential series to an adequately high order.

In order to gauge the roles of the various matrices appearing in the color trace, it is instructive to analyze the structure of the resummed cross section (19) in Mellin space after expansion to NLO:

$$\tilde{\omega}^{\rm resum}_{ab\to cd}\left(N,\Delta\eta,\alpha_s(\mu_R),\frac{\mu_R}{\hat{m}},\frac{\mu_F}{\hat{m}}\right) = \left(\frac{\alpha_s(\mu_R)}{\pi}\right)^2\left[{\rm Tr}\{H^{(0)}S^{(0)}\}_{ab\to cd}\left\{1+2b_0\alpha_s(\mu_R)\ln\frac{\mu_R^2}{\hat{m}^2}\right.\right.$$
$$+\frac{\alpha_s(\mu_R)}{\pi}\sum_{i=a,b,c,d}\left(A_i^{(1)}\ln^2\bar{N}+\frac{1}{4}A_i^{(1)}\zeta(2)+\left(A_i^{(1)}\ln\bar{N}+\frac{1}{2}B_i^{(1)}\right)\ln\frac{\mu_F^2}{\hat{m}^2}\right)\Big\}$$
$$\left.+\frac{\alpha_s(\mu_R)}{\pi}{\rm Tr}\Big\{-\left[H^{(0)}(\Gamma^{(1)})^\dagger S^{(0)}+H^{(0)}S^{(0)}\Gamma^{(1)}\right]\ln\bar{N}+H^{(1)}S^{(0)}+H^{(0)}S^{(1)}\Big\}_{ab\to cd}\right]+\mathcal{O}(\alpha_s^4) . \quad (38)$$

Here the term $\propto\zeta(2)$ arises from the coefficient $\tilde{R}_i$ in (26). We have anticipated the contributions by the functions ξ_R and ξ_F in (19) that will be specified in the next subsection. ξ_R yields the term involving the renormalization scale, and ξ_F contributes the ones $\propto B_i^{(1)}$, with

$$B_q^{(1)} = -\frac{3}{2}C_F , \qquad B_g^{(1)} = -2\pi b_0 . \quad (39)$$

The term ${\rm Tr}\{H^{(0)}S^{(0)}\}_{ab\to cd}$ in (38) is proportional to the LO function $\omega^{(0)}_{ab\to cd}(\Delta\eta)$ introduced in Eq. (10). In [16] (as in many previous studies of threshold resummation for hadronic hard-scattering), the combination ${\rm Tr}[H^{(1)}S^{(0)}+H^{(0)}S^{(1)}]$, which carries no dependence on N, was extracted as a whole by matching the expression in Eq. (38) to the NLO calculation at threshold. Of course, this is not sufficient for determining the full first-order matrices $H^{(1)}$ and $S^{(1)}$. However, it is a valid approach at NLL accuracy, where the three most dominant towers of logarithms are taken into account. For a given fixed-order expansion to $\mathcal{O}(\alpha_s^k)$, the following terms are under control:

$$\alpha_s^k\ \left\{\ln^{2k}\bar{N},\ \ln^{2k-1}\bar{N},\ \ln^{2k-2}\bar{N}\right\} . \quad (40)$$

It is straightforward to see that the hard and soft matrices will contribute to the third tower of threshold logarithms always in the combination ${\rm Tr}\{H^{(1)}S^{(0)}+H^{(0)}S^{(1)}\}_{ab\to cd}$ in the following way:

$$\left(\frac{\alpha_s}{\pi}\right)^k\frac{\sum_i A_i^{(1)}}{(k-1)!}\,{\rm Tr}\left\{H^{(1)}S^{(0)}+H^{(0)}S^{(1)}\right\}_{ab\to cd}\ln^{2k-2}\bar{N} . \quad (41)$$

Hence, to NLL, it is sufficient to know the combined expression of $H^{(1)}$ and $S^{(1)}$ instead of having to compute the full matrices separately. It is then legitimate to that order to approximate the

trace term in the resummed formula by

$$\mathrm{Tr}\left\{H\mathcal{S}_N^\dagger S\mathcal{S}_N\right\}_{ab\to cd,\,\mathrm{NLL}} = \left(1+\frac{\alpha_s}{\pi}\,C_{ab\to cd}^{(1),\,\mathrm{NLL}}\right)\,\mathrm{Tr}\left\{H^{(0)}\mathcal{S}_N^\dagger S^{(0)}\mathcal{S}_N\right\}_{ab\to cd}\,, \tag{42}$$

where

$$C_{ab\to cd}^{(1),\,\mathrm{NLL}}\left(\Delta\eta\right) \equiv \frac{\mathrm{Tr}\left\{H^{(1)}S^{(0)}+H^{(0)}S^{(1)}\right\}_{ab\to cd}}{\mathrm{Tr}\left\{H^{(0)}S^{(0)}\right\}_{ab\to cd}}\,. \tag{43}$$

This was the approach adopted in [16] and also, for example, in studies on single-inclusive hadron [37] or jet production [38].

On the other hand, in order to control the fourth tower of logarithms, $\alpha_s^k\,\ln^{2k-3}\bar{N}$, one needs to know $H^{(1)}$ and $S^{(1)}$ explicitly as they also appear separately in various combinations with the anomalous dimension matrices. Computation of the full matrices is therefore a necessary ingredient for NNLL resummation. Clearly, having the matrices at hand, one can compute also the known combination $\mathrm{Tr}\{H^{(1)}S^{(0)}+H^{(0)}S^{(1)}\}_{ab\to cd}$, which provides an important cross-check on them. We stress further that, in order to fully take into account also the fifth tower $\alpha_s^k\,\ln^{2k-4}\bar{N}$ at NNLL, one would need to know the full matrices $H^{(2)}$ and $S^{(2)}$ and perform a matching to NNLO. Although $H^{(2)}$ became available very recently [15], this is beyond the scope of the present work.

We finally note that a new feature which first appears at NNLL is that the hard-scattering matrix H obtains an imaginary part. This is due to the fact that H is constructed from virtual corrections to partonic $2\to 2$ scattering, which contain logarithms of ratios of space- and timelike invariants. We write

$$H = H_R + iH_I \tag{44}$$

with H_R and H_I real. It turns out that H_R is a symmetric matrix, whereas H_I is antisymmetric; see Section 3.2. Hence, the hard-scattering matrix H as a whole is hermitian, as it should be. The imaginary part H_I contributes to the resummed cross section due to the fact that the remaining terms inside the color trace in the resummed cross section (19), $M \equiv \mathrm{e}^{\Gamma^\dagger}S\mathrm{e}^{\Gamma}$, also develop an imaginary part since the anomalous dimension matrices are complex-valued [2, 9]. M is also hermitian as the soft matrix S is symmetric, and therefore we may also decompose $M = M_R + iM_I$ with M_R symmetric and M_I antisymmetric. The trace $\mathrm{Tr}\left\{HM\right\}$ is then real, as it must be, but both the real and imaginary parts of H, M contribute:

$$\mathrm{Tr}\left\{HM\right\} = \mathrm{Tr}\left\{H_RM_R\right\} - \mathrm{Tr}\left\{H_IM_I\right\}\,. \tag{45}$$

Note that the contribution by the imaginary part of H drops out from $\mathrm{Tr}[H^{(1)}S^{(0)}+H^{(0)}S^{(1)}]$, so that it is not present at NLL. Performing an analytical fixed-order expansion of our NNLL resummed result, we find that the imaginary parts of H and M first start to play a role at $\mathrm{N^3LO}$, where they contribute to the fifth tower, $\alpha_s^3\,\ln^2\bar{N}$. We note, however, that the imaginary parts of $\Gamma_{ab\to cd}$ also contribute to the real part of M, since $M = \mathrm{e}^{\Gamma^\dagger}S\mathrm{e}^{\Gamma}$. It turns out that they already appear in the *fourth* tower of logarithms. In this way we see that the imaginary parts of the various contributions are important ingredients of the NNLL resummed cross section.

3.1.3 Functions ξ_R and ξ_F

The N-independent function ξ_F^{abcd} in Eq. (19) addresses the factorization scale dependence of the cross section [2, 9, 10, 39]:

$$\ln \xi_F^{abcd}\left(\alpha_s(\mu_R), \frac{\mu_F}{\hat{m}}\right) = -\frac{1}{2}\sum_{i=a,b,c,d}\int_{\mu_F^2}^{\hat{m}^2}\frac{d\mu^2}{\mu^2}\frac{\alpha_s(\mu)}{\pi}B_i^{(1)}\,, \tag{46}$$

where we are summing over all four external partons. The coefficients $B_i^{(1)}$, which have been given in Eq. (39), correspond to the δ-function contributions to the corresponding LO diagonal parton-to-parton splitting functions and thus depend on whether the considered parton i is a quark or a gluon. As follows from [40], the function ξ_F^{abcd} takes into account all N-independent pieces corresponding to the evolution of parton distributions and fragmentation functions between scales μ_F and $\hat{m}$. Again its first-order contribution would explicitly appear in $H_{ab\to cd}^{(1)}$, from where it has been absorbed. It is straightforward to expand (46) to the desired NNLL accuracy.

ξ_R governs the renormalization scale dependence of the resummed cross section. This function was also introduced in [10]. ξ_R essentially serves to set the scale in the strong coupling constant in the overall factor α_s^2 (see Eq. (8)) of the cross section to $\hat{m}$:

$$\ln \xi_R\left(\alpha_s(\mu_R), \frac{\mu_R}{\hat{m}}\right) = 2\int_{\mu_R^2}^{\hat{m}^2}\frac{d\mu^2}{\mu^2}\beta(\alpha_s(\mu))\,. \tag{47}$$

Evaluating the integral while keeping only the first two terms in the QCD β-function,

$$\beta(\alpha_s) \equiv \frac{1}{\alpha_s}\frac{d\alpha_s}{d\log(\mu^2)} = -b_0\alpha_s - b_1\alpha_s^2 + \mathcal{O}(\alpha_s^3)\,, \tag{48}$$

and expanding the result up to second order in α_s, we find

$$\ln \xi_R\left(\alpha_s, \frac{\mu_R}{\hat{m}}\right) = 2b_0\alpha_s \ln\frac{\mu_R^2}{\hat{m}^2} + \alpha_s^2\left(2b_1\ln\frac{\mu_R^2}{\hat{m}^2} + b_0^2\ln^2\frac{\mu_R^2}{\hat{m}^2}\right)\,. \tag{49}$$

Here b_0, b_1 are as given in (30). The first term on the right reproduces the explicit μ_R-dependence of the first-order hard-scattering function that we have chosen to pull out of $H_{ab\to cd}^{(1)}$. The additional terms generated by this expression produce higher-order scale-dependent contributions that will occur in the perturbative series. When combined with resummation at NNLL level, they necessarily help to stabilize the cross section with respect to changes in μ_R, as we shall discuss in more detail now.

Following [41] and suppressing all arguments except for the renormalization scale, we write the perturbative expansion of a generic partonic cross section ω as

$$\omega = \sum_{k=0}^{\infty}\alpha_s^{k+2}(\mu_R)\,\omega^{(k)}(\mu_R)\,. \tag{50}$$

The LO coefficient $\omega^{(0)}$ is independent of μ_R; all higher-order terms depend on μ_R through the logarithm $L \equiv \ln(\mu_R^2/\hat{m}^2)$. Truncating the series at some fixed $k = n$, the uncertainty introduced

by the renormalization scale dependence is of the order of $\mathcal{O}(\alpha_s(\mu_R)^{n+3})$. In the following we consider as an example the renormalization scale dependence after truncation to next-to-next-to-leading order (NNLO), which is given by

$$\begin{aligned}\omega|_{\rm NNLO} &= \alpha_s^2(\mu_R)\,\omega^{(0)} + \alpha_s^3(\mu_R)\,\omega^{(1)}(\mu_R) + \alpha_s^4(\mu_R)\,\omega^{(2)}(\mu_R) \\ &= \alpha_s^2(\mu_R)\,\omega^{(0)} + \alpha_s^3(\mu_R)\,\left(\omega'^{(1)} + 2b_0\,L\,\omega^{(0)}\right) \\ &+ \alpha_s^4(\mu_R)\,\left(\omega'^{(2)} + 3b_0\,L\,\omega'^{(1)} + (3b_0^2\,L^2 + 2b_1\,L)\,\omega^{(0)}\right)\,, \end{aligned} \tag{51}$$

where the coefficients $\omega'^{(k)}$ denote the terms in $\omega^{(k)}$ that do not carry any dependence on μ_R. As is well-known, the μ_R-dependence of the NNLO cross section is entirely determined by the NLO terms in the perturbative expansion.

We may now compare the general expression in Eq. (51) to an NNLO expansion of the resummed cross section $\tilde{\omega}^{\rm resum}$ at either NLL or NNLL. First of all, we find that the NLO scale dependence and the contribution $(3b_0^2\,L^2 + 2b_1\,L)\,\omega^{(0)}$ at NNLO are entirely reproduced by the exponential ξ_R in Eqs. (47) and (49). The interesting term at NNLO is now the term $3b_0\,L\,\omega'^{(1)}$ in the last line. Out of the five towers of threshold logarithms that appear at NNLO, the renormalization scale dependence resides only in the lowest three. Indeed, as can be seen from the explicit NLO expansion given in Eq. (38), the coefficient $\omega'^{(1)}$ contains terms proportional to $\ln^2\bar{N}$, $\ln\bar{N}$, 1 which, at NNLO, correspond to the 3$^{\rm rd}$, 4$^{\rm th}$ and 5$^{\rm th}$ towers. If we now compare to the NNLO expansion of the *NLL*-resummed cross section, we find that only the scale dependence of the 3$^{\rm rd}$ tower is correctly reproduced. For the 4$^{\rm th}$ and 5$^{\rm th}$ tower, that are not fully taken into account at NLL, we find a factor of $2b_0\,L$ instead of $3b_0\,L$ multiplying the corresponding part of the coefficient $\omega'^{(1)}$. If instead resummation is performed at NNLL, the scale dependence in the 4$^{\rm th}$ tower is correctly reproduced as well, whereas in the 5$^{\rm th}$ tower the incorrect factor $2b_0\,L$ remains. (In addition, of course, the scale-independent coefficient $\omega'^{(2)}$ also changes). As it turns out, going from NLL to NNLL leads to a dramatic reduction of the renormalization scale uncertainty of the resummed cross section, as will be seen in our numerical studies in Sec. 4.

3.2 Hard-scattering function

In this Section we present our derivation of the matrices $H^{(1)}_{ab\to cd}$. We note that these were also determined in [24]; the results of our independent computation are in agreement with that reference. As the resulting expressions become rather lengthy in general, we present explicit results only for the simplest partonic channel, $qq' \to qq'$. For ease of notation, we will usually drop the ubiquitous subscript "$qq' \to qq'$" of the matrices. We also refer the reader to Ref. [10], where many details of the relevant color bases have been collected. In fact, for each partonic channel we adopt the corresponding color basis from that reference. We note that our choice differs from the one in [24], where an overcomplete basis was chosen for the $gg \to gg$ channel.

3.2.1 Color basis and lowest-order contribution

We consider the partonic process

$$q(p_1,a)q'(p_2,b) \to q(p_3,c)q'(p_4,d)\,, \tag{52}$$

where the p_i are the momenta of the incoming and outgoing quarks, and the indices a, b, c, d denote their color. Given the fact that the leading-order process has only a t-channel contribution, it is convenient to choose the t-channel octet-singlet color basis which leads to a simple form for the lowest-order hard-scattering matrix $H^{(0)}$. The contributing color tensors in this basis are given by (1=octet, 2=singlet)

$$\begin{aligned} \mathcal{C}_1 &\equiv T^g_{ca} T^g_{db} = \frac{1}{2}\left(\delta_{ad}\,\delta_{bc} - \frac{1}{N_c}\,\delta_{ac}\,\delta_{bd}\right) , \\ \mathcal{C}_2 &\equiv \delta_{ac}\delta_{bd} , \end{aligned} \tag{53}$$

where T^g is the generator in the fundamental representation and the indices a, b, c, d will be kept implicit throughout most of our discussion. The soft and hard functions become matrices in this basis, whose entries are determined as the coefficients multiplying the respective tensor structures. The elements of the leading-order contribution to the soft function $S^{(0)}$ in Eq. (32) are given by $(I, J = 1, 2)$

$$(S^{(0)})_{JI} \equiv \mathrm{Tr}[\mathcal{C}_J^\dagger \mathcal{C}_I] \equiv \sum_{a,b,c,d=1}^{N_c} \mathcal{C}_J^* \mathcal{C}_I \, . \tag{54}$$

In our basis one finds

$$S^{(0)} = \begin{pmatrix} \frac{N_c^2-1}{4} & 0 \\ 0 & N_c^2 \end{pmatrix} . \tag{55}$$

We next color-decompose the Born amplitude for the process as

$$M^{(0)} = \sum_I h_I^{(0)} \mathcal{C}_I \, . \tag{56}$$

Squaring the amplitude and summing (averaging) over external colors and helicities, we find

$$\frac{1}{4N_c^2} \sum_{a,b,c,d=1}^{N_c} |M^{(0)}|^2 = \frac{1}{4N_c^2} \sum_{a,b,c,d=1}^{N_c} \sum_{IJ} h_I^{(0)} h_J^{(0)*} \mathcal{C}_J^* \mathcal{C}_I = \frac{1}{4N_c^2} \sum_{IJ} h_I^{(0)} h_J^{(0)*} S_{JI}^{(0)} \equiv \mathrm{Tr}[H^{(0)} S^{(0)}] \, , \tag{57}$$

where

$$(H^{(0)})_{IJ} \equiv \frac{1}{4N_c^2}\, h_I^{(0)} h_J^{(0)*} \, . \tag{58}$$

While the matrix $H^{(0)}$ follows from a simple direct calculation, we extract it from the results of [21], since we can then follow the same strategy for the one-loop results given there. The color-decomposed tree-level four-point helicity amplitudes for $qq' \to qq'$ are given in [21] as

$$\begin{aligned} \mathcal{A}_{\text{tree}}^{\lambda\lambda'} &= \left(\delta_{ad}\,\delta_{bc} - \frac{1}{N_c}\,\delta_{ac}\,\delta_{bd}\right) a_{4;0}^{\lambda\lambda'} \\ &\equiv \mathcal{C}_1 \times \left(2 a_{4;0}^{\lambda\lambda'}\right) + \mathcal{C}_2 \times 0 \, , \end{aligned} \tag{59}$$

where $\lambda\lambda'$ denotes the helicity configuration of the initial partons. For a given pair of helicity settings we have $h_{I=1}^{(0)} = 2a_{4;0}$, $h_{I=2}^{(0)} = 0$. The squares of the two helicity amplitudes are

$$\begin{aligned} |a_{4;0}^{--}|^2 &= \frac{s^2}{t^2} \, , \\ |a_{4;0}^{-+}|^2 &= \frac{u^2}{t^2} \, , \end{aligned} \tag{60}$$

with the Mandelstam variables

$$\begin{aligned} s &= (p_1+p_2)^2 = \hat{m}^2 \,, \\ t &= (p_1-p_3)^2 = -\hat{m}^2 \frac{e^{-\Delta\eta}}{e^{\Delta\eta}+e^{-\Delta\eta}} \,, \\ u &= (p_1-p_4)^2 = -\hat{m}^2 \frac{e^{\Delta\eta}}{e^{\Delta\eta}+e^{-\Delta\eta}} \,. \end{aligned} \tag{61}$$

Averaging over external colors and helicities appropriately, following Eq. (57), we obtain the lowest-order hard-scattering matrix as

$$H^{(0)} = \begin{pmatrix} \frac{2}{N_c^2}\frac{s^2+u^2}{t^2} & 0 \\ 0 & 0 \end{pmatrix} \equiv \begin{pmatrix} h_0 & 0 \\ 0 & 0 \end{pmatrix} \,, \tag{62}$$

in agreement with [10]. As expected, its only entry is in the "octet-octet" corner, thanks to our choice of color basis.

3.2.2 Hard part at one loop

The hard-scattering matrix $H_{ab\to cd}$ is a perturbative function that contains all contributions associated with momenta of the order of the hard scale $\hat{m}$. Since in the threshold regime there is no phase space for hard on-shell radiation, only purely virtual contributions contribute to $H_{ab\to cd}$. Writing the virtual one-loop amplitude as (again we suppress the indices for the external particles)

$$M^{(1),\mathrm{virt}} = \sum_I \tilde{h}_I^{(1)} \mathcal{C}_I \,, \tag{63}$$

and considering the interference with the Born amplitude, the elements of the first-order contribution $H^{(1)}_{ab\to cd}$ are obtained from the finite part of

$$(\tilde{H}^{(1)})_{IJ} \equiv \frac{1}{4N_c^2}\left(\tilde{h}_I^{(1)} h_J^{(0)*} + h_I^{(0)} \tilde{h}_J^{(1)*}\right) \,. \tag{64}$$

Most of the one-loop amplitudes that we need are given in [21]. For the gluonic channel $gg\to gg$, we additionally use the results of [22, 23]. For the process $qq'\to qq'$, the one-loop four-point helicity amplitudes are given in [21] as

$$\begin{aligned} \mathcal{A}_{1\mathrm{loop}}^{\lambda\lambda'} &= \left(\delta_{ad}\,\delta_{bc} - \frac{1}{N_c}\,\delta_{ac}\,\delta_{bd}\right) a_{4;1}^{\lambda\lambda'} + \delta_{ad}\,\delta_{bc}\, a_{4;2}^{\lambda\lambda'} \\ &= \mathcal{C}_1 \times 2\left(a_{4;1}^{\lambda\lambda'} + a_{4;2}^{\lambda\lambda'}\right) + \mathcal{C}_2 \times \frac{1}{N_c} a_{4;2}^{\lambda\lambda'} \,. \end{aligned} \tag{65}$$

From this we can determine the $\tilde{h}_I^{(1)}$. Keeping in mind that we have pulled out an overall factor α_s/π in our definition of the hard-scattering matrix $H^{(1)}$, cf. Eq. (31), we have $\tilde{h}^{(1)}_{I=1} = 2(a^{\lambda\lambda'}_{4;1}+a^{\lambda\lambda'}_{4;2})$ and $\tilde{h}^{(1)}_{I=2} = a^{\lambda\lambda'}_{4;2}/N_c$. As shown in [21], the $a^{\lambda\lambda'}_{4;1}$, $a^{\lambda\lambda'}_{4;2}$ are proportional to the tree-level $a^{\lambda\lambda'}_{4;0}$ in (59) for each helicity configuration:

$$\begin{aligned} a_{4;1}^{\lambda\lambda'} &= C_\Gamma\, F_{4;1}^{\lambda\lambda'} a_{4;0}^{\lambda\lambda'} \,, \\ a_{4;2}^{\lambda\lambda'} &= C_\Gamma\, F_{4;2}^{\lambda\lambda'} a_{4;0}^{\lambda\lambda'} \,, \end{aligned} \tag{66}$$

where in our normalization

$$C_\Gamma \;=\; \frac{e^{\gamma_E \varepsilon}}{4}\,\frac{\Gamma^2(1-\varepsilon)\,\Gamma(1+\varepsilon)}{\Gamma(1-2\varepsilon)}\,. \tag{67}$$

Here dimensional regularization with $D = 4-2\varepsilon$ dimensions is used. The $F^{\lambda\lambda'}_{4;1}$, $F^{\lambda\lambda'}_{4;2}$ are functions of the Mandelstam variables. Using the shorthand notation

$$L(t) = \log\frac{-t}{s}\,,\quad L(u) = \log\frac{-u}{s}\,,\quad L(s) = -i\pi\,, \tag{68}$$

we have from [21]:

$$\begin{aligned}
F^{--}_{4;1} &= N_c\left[-\frac{2}{\varepsilon^2}-\frac{3}{\varepsilon}+2\frac{L(s)}{\varepsilon}+L^2(t)-\frac{2}{3}L(t)\,(1+3L(s))+\frac{13}{9}+\pi^2\right]+N_f\left[\frac{2}{3}L(t)-\frac{10}{9}\right]\\
&\quad -\frac{1}{N_c}\left[-\frac{2}{\varepsilon^2}-\frac{3}{\varepsilon}-\frac{2}{\varepsilon}(L(s)-L(t)-L(u))-8-L^2(t)+\frac{u^2-s^2}{2s^2}\left((L(t)-L(u))^2+\pi^2\right)\right.\\
&\quad \left.+2L(t)(1+L(s)-L(u))-\frac{1}{s}(uL(t)+tL(u))\right]+4\pi b_0\log\left(\frac{\mu_R^2}{\hat m^2}\right)\,,\\
F^{-+}_{4;1} &= N_c\left[-\frac{2}{\varepsilon^2}-\frac{3}{\varepsilon}+2\frac{L(s)}{\varepsilon}+L^2(t)-\frac{2}{3}L(t)\,(1+3L(s))+\frac{13}{9}+\pi^2\right]+N_f\left[\frac{2}{3}L(t)-\frac{10}{9}\right]\\
&\quad -\frac{1}{N_c}\left[-\frac{2}{\varepsilon}-\frac{3}{\varepsilon}-\frac{2}{\varepsilon}(L(s)-L(t)-L(u))-8-L^2(t)+L(t)(3+2L(s)-2L(u))\right]\\
&\quad +\left(N_c+\frac{1}{N_c}\right)\left[\frac{s^2-u^2}{2u^2}(L^2(t)-2L(s)L(t))+\frac{t}{u}(L(t)-L(s))\right]+4\pi b_0\log\left(\frac{\mu_R^2}{\hat m^2}\right)\,,\\
F^{--}_{4;2} &= 2C_F\left[\frac{2}{\varepsilon}(L(u)-L(s))+\frac{u^2-s^2}{2s^2}\left(L^2(t)+L^2(u)+\pi^2\right)+\frac{t}{s}(L(t)-L(u))+2L(s)L(t)\right.\\
&\quad \left.-\frac{u^2+s^2}{s^2}L(t)L(u)\right]\,,\\
F^{-+}_{4;2} &= 2C_F\left[\frac{2}{\varepsilon}(L(u)-L(s))-\frac{s^2-u^2}{2u^2}L^2(t)-\frac{t}{u}(L(t)-L(s))-2L(t)L(u)+\frac{s^2+u^2}{u^2}L(t)L(s)\right]\,.
\end{aligned} \tag{69}$$

Note that the loop corrections have imaginary parts arising from the analytic continuation of Mandelstam variables into the physical region $s>0;\ t,u<0$. They appear in the finite part as well as in the pole contributions.

From this we can construct the matrix $\tilde H^{(1)}$ defined in Eq. (64) as

$$\tilde H^{(1)} = \frac{C_\Gamma}{4N_c^2}\begin{pmatrix} 16\left(\mathcal{R}e\left(F^{--}_{4;2}+F^{--}_{4;1}\right)\frac{s^2}{t^2}+\mathcal{R}e\left(F^{-+}_{4;2}+F^{-+}_{4;1}\right)\frac{u^2}{t^2}\right) & \frac{4}{N_c}\left(F^{--*}_{4;2}\frac{s^2}{t^2}+F^{-+*}_{4;2}\frac{u^2}{t^2}\right)\\ \frac{4}{N_c}\left(F^{--}_{4;2}\frac{s^2}{t^2}+F^{-+}_{4;2}\frac{u^2}{t^2}\right) & 0\end{pmatrix}\,. \tag{70}$$

The full expression for this matrix is rather lengthy. It has the following explicit structure:

$$\begin{aligned}
\tilde H^{(1)} &= \frac{1}{2}\left[\left(-\frac{4C_F}{\varepsilon^2}-\frac{6C_F}{\varepsilon}\right)H^{(0)}-\frac{L(s)}{\varepsilon}\frac{C_F}{N_c}\begin{pmatrix}0&-1\\1&0\end{pmatrix}-\frac{2}{\varepsilon}L(t)\frac{h_0}{N_c}\begin{pmatrix}1&0\\0&0\end{pmatrix}\right.\\
&+\left.\frac{1}{\varepsilon}L(u)\frac{h_0}{N_c}\begin{pmatrix}2(N_c^2-2)&C_F\\C_F&0\end{pmatrix}+4\pi b_0\log\left(\frac{\mu_R^2}{\hat m^2}\right)H^{(0)}\right]+\,H^{(1)}\,,
\end{aligned} \tag{71}$$

where h_0 and $H^{(0)}$ have been given in (62). Following [42], we have identified the finite part in the last line with the first-order correction to the hard-scattering matrix. This finite part is a function of the Mandelstam variables only. As one can see, the explicit dependence on the renormalization scale μ_R has been separated from $H^{(1)}$. It is proportional to $H^{(0)}$ and therefore fully taken into account by the exponential ξ_R in Eq. (47), as discussed in Sec. 3.1.

To present our final results for $H^{(1)}$, we adopt the notation of Ref. [24], where the matrix was derived in the context of the soft-collinear effective theory. We find full agreement with the result in their Eq. (39):

$$\begin{aligned}
\left(H^{(1)}\right)_{11} &= \mathcal{R}e\left\{\frac{1}{2N_c^2}\Big[\frac{s^2+u^2}{t^2}\left(-4C_F L(t)^2+2X_1(s,t,u)L(t)+2Y\right)\right.\\
&\qquad\left.+\frac{s^2}{t^2}(C_A-4C_F)Z(s,t,u)-\frac{u^2}{t^2}(2C_A-4C_F)Z(u,t,s)\Big]\right\},\\
\left(H^{(1)}\right)_{21} &= \frac{1}{2N_c^2}\Big[\frac{s^2+u^2}{t^2}X_2(s,t,u)L(t)-\frac{s^2}{t^2}\frac{C_F}{2C_A}Z(s,t,u)+\frac{u^2}{t^2}\frac{C_F}{2C_A}Z(u,t,s)\Big],\\
\left(H^{(1)}\right)_{12} &= \left(H^{(1)}\right)^*_{21},\\
\left(H^{(1)}\right)_{22} &= 0,
\end{aligned} \tag{72}$$

with [24]

$$\begin{aligned}
X_1(s,t,u) &= 6C_F-4\pi b_0+8C_F[L(s)-L(u)]-2C_A[2L(s)-L(t)-L(u)],\\
X_2(s,t,u) &= \frac{2C_F}{C_A}[L(s)-L(u)],\\
Y &= C_A\left(\frac{10}{3}+\pi^2\right)+C_F\left(\frac{\pi^2}{3}-16\right)+\frac{5}{3}4\pi b_0,\\
Z(s,t,u) &= \frac{t}{s}\left(\frac{t+2u}{s}[L(u)-L(t)]^2+2[L(u)-L(t)]+\pi^2\frac{t+2u}{s}\right).
\end{aligned} \tag{73}$$

There are several ways of checking the validity of the results. The simplest one is to compute

$$\mathrm{Tr}\left[\tilde{H}^{(1)}\,S^{(0)}\right], \tag{74}$$

which should reproduce the known one-loop virtual correction to $qq'\to qq'$ scattering given in [21]. This indeed turns out to be the case. Since $S^{(0)}$ is diagonal in our basis, this provides a check on the diagonal elements of $H^{(1)}$.

We also note that the pole terms of the NLO virtual amplitudes $M^{(1),\mathrm{virt}}$ in (63), including their imaginary parts, have been predicted in [42, 43] to be given by

$$\tilde{h}_I^{(1)}|_{\substack{\mathrm{pole}\\ \mathrm{terms}}} = \frac{1}{2}\left[-C_F\left(\frac{2}{\varepsilon^2}+\frac{3}{\varepsilon}\right)\mathbb{1}+\frac{1}{\varepsilon}\Gamma^{(1)}_{qq'\to qq'}\right]_{IJ}h_J^{(0)}, \tag{75}$$

where $\mathbb{1}$ denotes the 2×2 unit matrix and $\Gamma^{(1)}_{qq'\to qq'}$ is the soft anomalous dimension matrix introduced in (34) which possesses imaginary parts (the explicit result for $\Gamma^{(1)}_{qq'\to qq'}$ is given in Eq. (85) below). We have verified that this correctly reproduces the pole terms in the $\tilde{h}^{(1)}_I$.

In the way described in this subsection we have determined the one-loop hard-scattering matrix for each partonic channel contributing to di-hadron production. As one can see in Eqs. (71),(72), for $qq' \to qq'$ the final expression always contains the squares of the tree-level helicity amplitudes $a_{4;0}$. This becomes different for partonic channels involving both external quarks and gluons.

3.3 Soft function

We now turn to the computation of the first-order correction $S^{(1)}_{ab\to cd}$ to the soft function in Eq. (32). Again we present explicit results only for the qq' channel, although we have of course considered all partonic channels. In fact, in the course of the study of qq' scattering we find a general construction rule for the soft matrix $S^{(1)}_{ab\to cd}$ that turns out to be applicable to all partonic channels.

3.3.1 Color structure of diagrams in the eikonal approximation

In order to to compute the soft matrix at NLO for qq' scattering, we need to consider the process $q(p_1) + q'(p_2) \to q(p_3) + q'(p_4) + g(k)$, where g denotes a radiated gluon with soft momentum k. The diagrams are treated in the eikonal approximation, decomposed according to our color basis. They are shown in Fig. 1. The blobs on either side of the cut denote a Born hard part that can be a color-octet or a singlet. There are six diagrams labeled "34" or "12" for example, depending on the external legs between which the additional gluon is exchanged. Eventually, all contributions must be summed. Using the notation of the previous subsection, each of the diagrams in Fig. 1 has the structure

$$\sum_{IJ} h^{(0)}_I h^{(0)*}_J \, (\mathcal{R}_{ij})_{JI} \, I_{ij} \;, \tag{76}$$

where ij labels the diagram, I_{ij} is an integral over the eikonal factor corresponding to the diagram that we will specify below, and the $(\mathcal{R}_{ij})_{JI}$ form a 2×2 matrix with entries labeled by JI =octet-octet, singlet-octet, etc. For example, for the "octet-octet" entry of $\mathcal{R}_{34}$ we have

$$\begin{aligned}
(\mathcal{R}_{34})_{\substack{J=\text{octet}\\ I=\text{octet}}} &= \sum_{\substack{a,b,c,d,c',d'\\ g,g_1,g_2}} T^{g_2}_{bd'} T^{g_2}_{ac'} \; T^{g}_{d'd} T^{g}_{c'c} \; T^{g_1}_{db} T^{g_1}_{ca} \\
&= \sum_{g,g_1,g_2} \mathrm{Tr}[T^{g_2} T^{g} T^{g_1}] \, \mathrm{Tr}[T^{g_2} T^{g} T^{g_1}] \\
&= -\frac{N_c^2 - 1}{4N_c} = -\frac{C_F}{2} \;.
\end{aligned} \tag{77}$$

Here g corresponds to the color of the gluon exchanged between the external legs, while g_1 and g_2 are those for the gluons in the amplitudes on the two sides of the cut. Computing in this way the

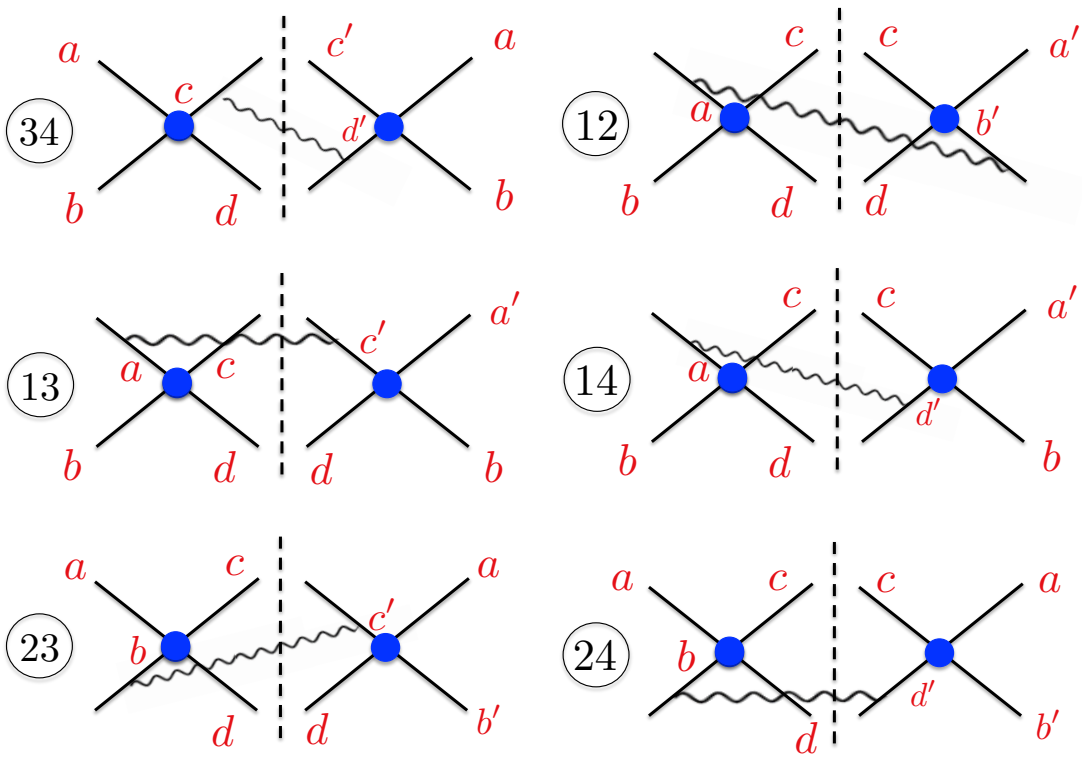

Figure 1: Diagrams relevant for the calculation of the NLO soft matrix $S^{(1)}$. The blobs represent a Born amplitude and the letters are color indices.

matrices $\mathcal{R}_{ij}$ for all diagrams, we find:

$$\begin{aligned}
\mathcal{R}_{12} &= \mathcal{R}_{34} = \frac{C_F}{2}\begin{pmatrix} -1 & N_c \\ N_c & 0 \end{pmatrix}, \\
\mathcal{R}_{13} &= \mathcal{R}_{24} = \frac{C_F}{2}\begin{pmatrix} -\frac{1}{2} & 0 \\ 0 & 2N_c^2 \end{pmatrix}, \\
\mathcal{R}_{14} &= \mathcal{R}_{23} = \frac{C_F}{2}\begin{pmatrix} \frac{1}{2}(N_c^2-2) & N_c \\ N_c & 0 \end{pmatrix}.
\end{aligned} \tag{78}$$

For the sum of all diagrams we thus have

$$\sum_{ij} \mathcal{R}_{ij}\, I_{ij} = \frac{C_F}{2}\begin{pmatrix} \frac{1}{2}(I_{13}+I_{24}) - I_{12} - I_{34} - \frac{N_c^2-2}{2}(I_{14}+I_{23}) & N_c(I_{12}+I_{34}-I_{14}-I_{23}) \\ N_c(I_{12}+I_{34}-I_{14}-I_{23}) & -2N_c^2(I_{13}+I_{24}) \end{pmatrix}. \tag{79}$$

We note that the eikonal factor for the interference between initial- and final-state emission has an extra minus sign which we included here.

3.3.2 Integrals I_{ij}

Next, we need to specify and compute the I_{ij}. They are essentially given by eikonal factors integrated over the gluon phase space. They are normalized relative to the Born cross section.

Adopting the three-particle phase space in $d = 4-2\varepsilon$ dimensions from [16] (see also [12]), one has

$$I_{ij} = -\frac{\alpha_s}{\pi}\frac{s}{4\pi}e^{\varepsilon\gamma_E}\frac{\Gamma(1-\varepsilon)}{\Gamma(1-2\varepsilon)}\int_0^1 d\hat{\tau}\,\hat{\tau}^{-\varepsilon}(1-\hat{\tau})^{1-2\varepsilon}\int d\Omega\,\frac{p_i\cdot p_j}{(p_i\cdot k)(p_j\cdot k)}\,, \tag{80}$$

where

$$\int d\Omega = \int_0^\pi d\psi \sin^{1-2\varepsilon}\psi \int_0^\pi d\theta\, \sin^{-2\varepsilon}\theta\,. \tag{81}$$

We work in the c.m.s. of the incoming partons; ψ and θ are the gluon's polar and azimuthal angles relative to the plane defined by the directions of incoming and outgoing hard partons. The relevant angular integrals are well-known [44]:

$$\begin{aligned}\int d\Omega\,&\frac{1}{(1-\cos\psi)^j(1-\cos\psi\cos\chi-\sin\psi\cos\theta\sin\chi)^k}\\ &= 2\pi\frac{\Gamma(1-2\varepsilon)}{\Gamma(1-\varepsilon)^2}\,2^{-j-k}\,B(1-\varepsilon-j,1-\varepsilon-k)\,{}_2F_1\left(j,k,1-\varepsilon,\cos^2\frac{\chi}{2}\right)\,,\end{aligned} \tag{82}$$

with the Hypergeometric function ${}_2F_1$. Performing the integrations over $d\Omega$, but leaving the integration over $\hat{\tau}$ (or, equivalently, gluon energy) aside for the moment, we find near threshold

$$\begin{aligned}\frac{dI_{12}}{d\hat{\tau}} &= \frac{dI_{34}}{d\hat{\tau}} = -\frac{\alpha_s}{\pi}\left[\left(\frac{1}{\varepsilon^2}-\frac{\pi^2}{4}\right)\delta(1-\hat{\tau}) - \frac{2}{\varepsilon}\frac{1}{(1-\hat{\tau})_+} + 4\left(\frac{\ln(1-\hat{\tau})}{1-\hat{\tau}}\right)_+\right]\,,\\ \frac{dI_{13}}{d\hat{\tau}} &= \frac{dI_{24}}{d\hat{\tau}} = -\frac{\alpha_s}{\pi}\left[\left(\frac{1}{\varepsilon^2}-\frac{\pi^2}{4}-\frac{1}{\varepsilon}\ln\left(-\frac{t}{s}\right)-\mathrm{Li}_2\left(-\frac{u}{t}\right)\right)\delta(1-\hat{\tau})\right.\\ &\qquad\left.+2\left(-\frac{1}{\varepsilon}+\ln\left(-\frac{t}{s}\right)\right)\frac{1}{(1-\hat{\tau})_+} + 4\left(\frac{\ln(1-\hat{\tau})}{1-\hat{\tau}}\right)_+\right]\,,\\ \frac{dI_{23}}{d\hat{\tau}} &= \frac{dI_{14}}{d\hat{\tau}} = \frac{dI_{13}}{d\hat{\tau}}\Big|_{t\leftrightarrow u}\,,\end{aligned} \tag{83}$$

where Li_2 denotes the Dilogarithm function.

3.3.3 Extraction of $S^{(1)}$

Combining Eqs. (79) and (83), we obtain

$$\begin{aligned}\sum_{ij}\mathcal{R}_{ij}\frac{dI_{ij}}{d\hat{\tau}}\\ = \; C_F\frac{\alpha_s}{\pi}\Bigg[&\left\{\delta(1-\hat{\tau})\left(\frac{1}{2\varepsilon^2}-\frac{\pi^2}{8}\right)-\frac{1}{\varepsilon}\frac{1}{(1-\hat{\tau})_+}+2\left(\frac{\ln(1-\hat{\tau})}{1-\hat{\tau}}\right)_+\right\}\begin{pmatrix}N_c^2-1 & 0\\ 0 & 4N_c^2\end{pmatrix}\\ &+\left\{\delta(1-\hat{\tau})\frac{1}{2\varepsilon}-\frac{1}{(1-\hat{\tau})_+}\right\}\begin{pmatrix}\ln\left(-\frac{t}{s}\right)+(2-N_c^2)\ln\left(-\frac{u}{s}\right) & -2N_c\ln\left(-\frac{u}{s}\right)\\ -2N_c\ln\left(-\frac{u}{s}\right) & -4N_c^2\ln\left(-\frac{t}{s}\right)\end{pmatrix}\\ &+\delta(1-\hat{\tau})\frac{1}{2}\begin{pmatrix}\mathrm{Li}_2\left(-\frac{u}{t}\right)+(2-N_c^2)\,\mathrm{Li}_2\left(-\frac{t}{u}\right) & -2N_c\,\mathrm{Li}_2\left(-\frac{t}{u}\right)\\ -2N_c\,\mathrm{Li}_2\left(-\frac{t}{u}\right) & -4N_c^2\,\mathrm{Li}_2\left(-\frac{u}{t}\right)\end{pmatrix}\Bigg]\,.\end{aligned} \tag{84}$$

In the first term we recognize the lowest-order soft matrix of Eq. (55). The matrix in the second term has a direct relation to the one-loop soft anomalous dimension matrix $\Gamma^{(1)}_{qq'\to qq'}$ introduced in (34),(35), which in our color basis is given by [10]

$$\Gamma^{(1)}_{qq'\to qq'} = \begin{pmatrix} \frac{1}{N_c}(2S-T-U)+2C_F U & 2(U-S) \\ \frac{C_F}{N_c}(U-S) & 2C_F T \end{pmatrix}, \tag{85}$$

with[‡]

$$S = 0, \quad T = \ln\left(\frac{-t}{s}\right) + i\pi, \quad U = \ln\left(\frac{-u}{s}\right) + i\pi\,. \tag{86}$$

One easily checks that the matrix in the second line of (84) is given by $-[(\Gamma^{(1)})^\dagger S^{(0)} + S^{(0)}\Gamma^{(1)}]/C_F$. Hence, we have after some reordering of terms:

$$\begin{aligned} \sum_{ij} \mathcal{R}_{ij}\,\frac{dI_{ij}}{d\hat{\tau}} \;=\; & \frac{\alpha_s}{\pi}\Bigg[\delta(1-\hat{\tau})\,\left\{\frac{2C_F}{\varepsilon^2}S^{(0)} - \frac{1}{2\varepsilon}\,\left[(\Gamma^{(1)})^\dagger S^{(0)} + S^{(0)}\Gamma^{(1)}\right]\right\} \\ & - \frac{4C_F}{\varepsilon}\,\frac{1}{(1-\hat{\tau})_+}\,S^{(0)} + 8C_F\left(\frac{\ln(1-\hat{\tau})}{1-\hat{\tau}}\right)_+ S^{(0)} + \frac{1}{(1-\hat{\tau})_+}\,\left[(\Gamma^{(1)})^\dagger S^{(0)} + S^{(0)}\Gamma^{(1)}\right] \\ & + \frac{C_F}{2}\delta(1-\hat{\tau})\left\{\begin{pmatrix} \mathrm{Li}_2\left(-\frac{u}{t}\right) + (2-N_c^2)\,\mathrm{Li}_2\left(-\frac{t}{u}\right) & -2N_c\,\mathrm{Li}_2\left(-\frac{t}{u}\right) \\ -2N_c\,\mathrm{Li}_2\left(-\frac{t}{u}\right) & -4N_c^2\,\mathrm{Li}_2\left(-\frac{u}{t}\right) \end{pmatrix} - \pi^2 S^{(0)}\right\}\Bigg]\,. \end{aligned} \tag{87}$$

Each of the terms in this equation has a transparent interpretation. The pole terms $\propto \delta(1-\hat{\tau})$ in the first line will be canceled by corresponding terms in the virtual correction; see Eq. (75). The single pole term $\propto 1/(1-\hat{\tau})_+$ will be canceled by collinear factorization in the eikonal approximation, as described in the Appendix. The next two terms precisely match the threshold logarithms at NLO, as becomes evident by going to Mellin-moment space and comparing to (38). The remaining term involves the one-loop soft matrix we are interested in. More precisely, since $S^{(1)}$ appears in the Mellin-space expression for the resummed cross section, and since the moments of $(\ln(1-\hat{\tau})/(1-\hat{\tau}))_+$ are given by $\frac{1}{2}(\ln^2\bar{N} + \pi^2/6)$ (up to corrections suppressed as $1/N$), all terms $\propto \pi^2$ match when comparing to (38), and we are just left with

$$S^{(1)} \;=\; \frac{C_F}{2}\begin{pmatrix} \mathrm{Li}_2\left(-\frac{u}{t}\right) + (2-N_c^2)\,\mathrm{Li}_2\left(-\frac{t}{u}\right) & -2N_c\,\mathrm{Li}_2\left(-\frac{t}{u}\right) \\ -2N_c\,\mathrm{Li}_2\left(-\frac{t}{u}\right) & -4N_c^2\,\mathrm{Li}_2\left(-\frac{u}{t}\right) \end{pmatrix}. \tag{88}$$

This is our final result for the one-loop soft matrix for this process. A powerful check on the result comes from comparison with the full cross section at NLO: Inserting our $S^{(1)}$ along with $H^{(1)}$ from Eq. (72) into (38), we verify that the resulting expression correctly reproduces all threshold logarithms *and all constant terms* in the NLO partonic cross section.

As it turns out, we can give a very simple rule for obtaining $S^{(1)}$ directly from $S^{(0)}$ and the anomalous dimension matrix $\Gamma^{(1)}$. This becomes already evident from comparison of the two

[‡]An equally possible choice is $S = -i\pi, T = \ln\left(\frac{-t}{s}\right), U = \ln\left(\frac{-u}{s}\right)$, which matches the logarithms in Eq. (68). One easily checks that $\Gamma^{(1)}_{qq'\to qq'}$ differs for the two choices only by a term proportional to the unit matrix which commutes with all other matrices and hence cancels in the final result. This holds true for all partonic channels. Note that even for the resummed cross section only the combination $\mathrm{e}^{\Gamma^\dagger} S \mathrm{e}^{\Gamma}$ contributes.

matrices in the second and third lines of (84): They have identical structure, except that each logarithm has to be replaced by a dilogarithm with suitably modified argument,

$$\begin{aligned} \ln\left(-\frac{t}{s}\right) &\to \mathrm{Li}_2\left(-\frac{u}{t}\right) , \\ \ln\left(-\frac{u}{s}\right) &\to \mathrm{Li}_2\left(-\frac{t}{u}\right) . \end{aligned} \tag{89}$$

The deeper reason for this is of course that already in the integrals (83) the logarithm and the dilogarithm always appear in the same ratio in the term $\propto \delta(1-\hat{\tau})$. Since we know how the matrix in the second line is expressed in terms of $S^{(0)}$ and $\Gamma^{(1)}$, we also know how to construct $S^{(1)}$: Compute the combination $-1/2\left((\Gamma^{(1)})^\dagger S^{(0)} + S^{(0)}\Gamma^{(1)}\right)$ and substitute each logarithm according to (89). As the integrals I_{ij} are the same no matter which process we are considering, this simple construction rule works for all partonic channels. All necessary ingredients, the $\Gamma^{(1)}_{ab\to cd}$ and the $S^{(0)}_{ab\to cd}$, may be found in the Appendix of Ref. [10]; we therefore do not present the explicit expressions for the resulting $S^{(1)}_{ab\to cd}$ for all the other channels, which become rather lengthy. It is likely that the simple rule we find is a special property of the pair mass kinematics we are considering here.

3.4 Inverse Mellin and Fourier transforms and matching procedure

In order to produce phenomenological results for the resummed case, we need to perform inverse Mellin transform and Fourier transforms. The Mellin inverse requires a prescription for dealing with the singularity in the perturbative strong coupling constant in the NNLL expansions of the resummed exponents. As in [16] we will use the *Minimal Prescription* developed in [45], which relies on use of the NNLL expanded forms given in Sec. 3.1 and on choosing a Mellin contour in complex-N space that lies to the *left* of the poles at $\lambda = 1/2$ and $\lambda = 1$ in the Mellin integrand. The function $\Omega_{H_1H_2\to cd}$ in (15) is obtained as [16]

$$\begin{aligned} \Omega^{\mathrm{resum}}_{H_1H_2\to cd}\left(\tau', \Delta\eta, \bar{\eta}, \alpha_s(\mu_R), \frac{\mu_R}{\hat{m}}, \frac{\mu_F}{\hat{m}}\right) &= \frac{1}{2\pi}\int_{-\infty}^{\infty} d\nu\, \mathrm{e}^{-i\nu\bar{\eta}} \int_{C_{MP}-i\infty}^{C_{MP}+i\infty} \frac{dN}{2\pi i}\, (\tau')^{-N} \\ &\times \sum_{ab} \tilde{f}_a^{H_1}(N+1+i\nu/2,\mu_F)\tilde{f}_b^{H_2}(N+1-i\nu/2,\mu_F)\, \tilde{\omega}^{\mathrm{resum}}_{ab\to cd}\left(N,\nu,\Delta\eta,\alpha_s(\mu_R),\frac{\mu_R}{\hat{m}},\frac{\mu_F}{\hat{m}}\right), \end{aligned} \tag{90}$$

with a suitable Mellin contour consistent with the minmal prescription. As shown in [16], it is straightforward to perform the convolution of the inverted resummed $\Omega^{\mathrm{resum}}_{H_1H_2\to cd}$ with the fragmentation functions, as given by (14).

As in [16], we match the resummed cross section to the full NLO one, by expanding the resummed cross section to $\mathcal{O}(\alpha_s^3)$, subtracting the expanded result from the resummed one, and adding the full NLO cross section:

$$d\sigma^{\mathrm{match}} = \left(d\sigma^{\mathrm{resum}} - d\sigma^{\mathrm{resum}}\Big|_{\mathcal{O}(\alpha_s^3)}\right) + d\sigma^{\mathrm{NLO}} . \tag{91}$$

For the NLO cross section we use the results of [46]. In this way, NLO is taken into account in full, and the soft-gluon contributions beyond NLO are resummed in the way described above. Of

course, for a full NNLL resummed cross section one would prefer to match to an NNLO calculation, which however is not available for this observable yet.

4 Phenomenological results

We now examine the numerical effects of our approximate NNLL resummation in comparison to the NLL and NLO results shown in [16]. Since the NNLL effects are generally rather similar for the experimental situations considered in [16], we show only two representative examples here. We will also make predictions for the di-hadron cross section at RHIC, where one would expect the effects of resummation to be smaller.

Our examples from [16] concern the NA24 [17] and the CCOR [20] $pp \to \pi^0\pi^0$ scattering experiments. The fixed-target experiment NA24 recorded data at a beam energy of $E_p = 300$ GeV, while CCOR operated at the ISR collider at $\sqrt{S} = 62.4$ GeV. Both experiments employed the cuts $p_T^{\rm pair} < 1$ GeV, $|Y| < 0.35$, and $|\cos\theta^*| < 0.4$. Here, $p_T^{\rm pair}$ and Y are the transverse momentum and rapidity of the pion pair, respectively, which are given in terms of the individual pion transverse momenta $p_{T,i}$ and of $\Delta\eta, \bar{\eta}$ in (4) by

$$\begin{aligned} p_T^{\rm pair} &= |p_{T,1} - p_{T,2}| \,, \\ Y &= \bar{\eta} - \frac{1}{2}\ln\left(\frac{p_{T,1}\,{\rm e}^{-\Delta\eta} + p_{T,2}\,{\rm e}^{\Delta\eta}}{p_{T,1}\,{\rm e}^{\Delta\eta} + p_{T,2}\,{\rm e}^{-\Delta\eta}}\right) \,, \end{aligned} \tag{92}$$

where LO kinematics have been assumed as appropriate in the threshold regime. Furthermore, $\cos\theta^*$ is the cosine of the scattering angle in the partonic c.m.s. and is for LO kinematics given by

$$\cos\theta^* = \frac{1}{2}\left(\frac{p_{T,1}}{p_{T,2} + p_{T,1}\cosh(2\Delta\eta)} + \frac{p_{T,2}}{p_{T,1} + p_{T,2}\cosh(2\Delta\eta)}\right)\sinh(2\Delta\eta) \,. \tag{93}$$

For details on the kinematical variables, see [16]. Thanks to our way of organizing the threshold resummed cross section, inclusion of cuts on any of these variables is straightforward.

In all our calculations, we use the CTEQ6M5 set of parton distribution functions [47], along with its associated value of the strong coupling constant. As compared to our results in [16], we update to the latest "de Florian-Sassot-Stratmann" (DSS) set of fragmentation functions [48]. We note that one might object that the use of NLO parton distribution functions and fragmentation functions is not completely justified for obtaining NNLL resummed predictions. However, since anyway fragmentation functions evolved at NNLO are not available yet, we have decided to stick to NLO functions throughout. As in [16], we choose the renormalization and factorization scales to be equal, $\mu_R = \mu_F \equiv \mu$, and we give them the values M and $2M$, in order to investigate the scale dependence of the results.

Figure 2 shows the comparison to the NA24 [17] data. As known from [16], the full NLO cross section and the first-order expansion of the resummed expression, that is, the last two terms in Eq. (91), agree to a remarkable degree. Their difference actually never exceeds 1% for the kinematics relevant for NA24. We recall these results by the dashed lines and the crosses in the figure. They provide confidence that the soft-gluon terms constitute the dominant part of the cross section, so that their resummation is sensible. The dot-dashed lines in the figure present the NLL

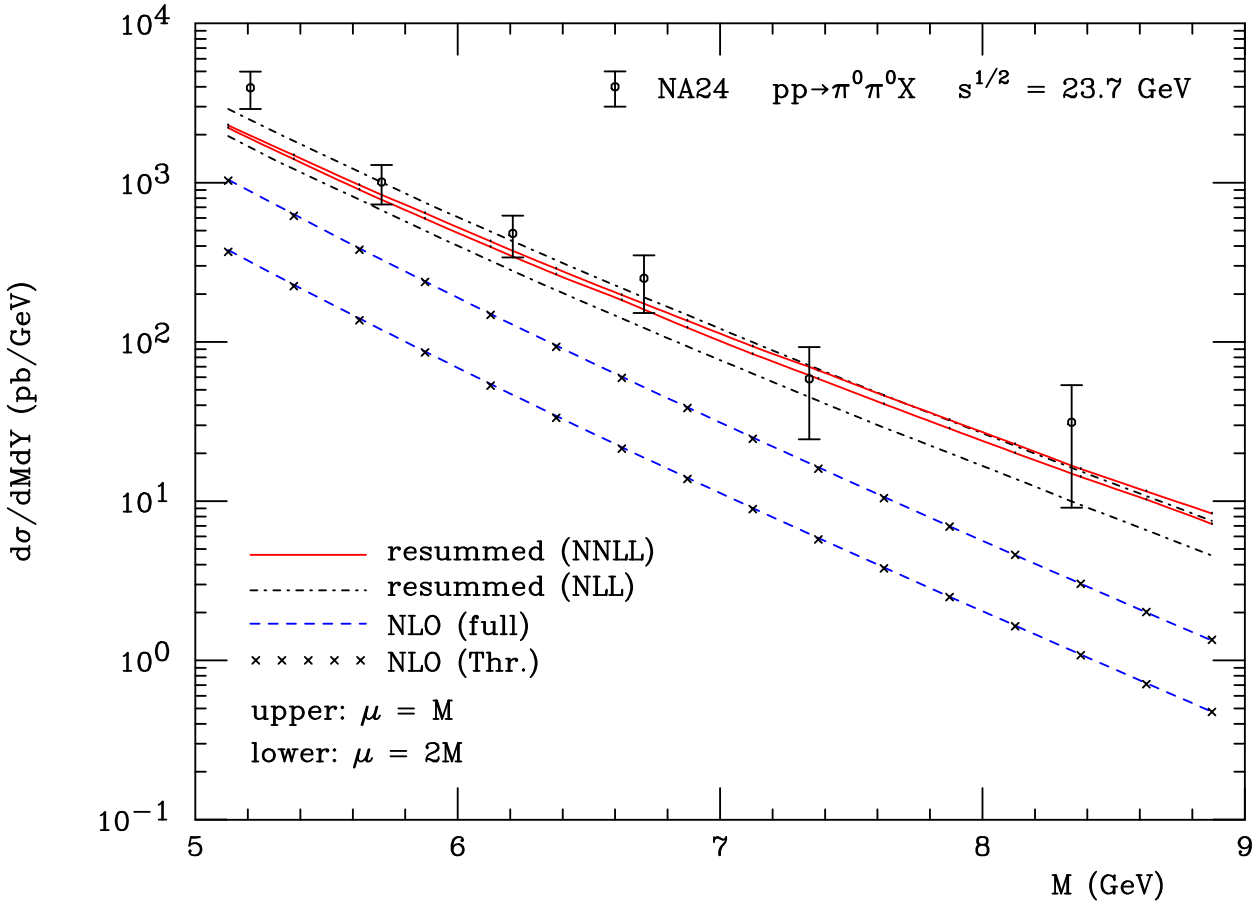

Figure 2: Comparison of NLO (dashed), NLL resummed (dot-dashed) and NNLL resummed (solid) calculations of the cross section for $pp \to \pi^0\pi^0 X$ to the NA24 data [17], for two different choices of the renormalization and factorization scales, $\mu_R = \mu_F = M$ (upper lines) and $\mu_R = \mu_F = 2M$ (lower lines). The crosses display the NLO $\mathcal{O}(\alpha_s)$ expansion of the resummed cross section.

results, computed by dropping all NNLL terms and matching to NLO via Eqs. (42),(43), as in [16]. As found there, resummation leads to a significant enhancement of the theoretical prediction and provides a much better description of the NA24 data [17] than for the NLO calculation. Finally, the two solid lines show our NNLL resummed results. The key observations are that the two NNLL results for scales $2M$ and M are very close together and both roughly fall within the "band" spanned by the two NLL results for the two scales. One also notices that the NNLL curves have a slope somewhat less steep than the NLL ones. Given the relatively large uncertainties of the data, it is fair to say that the main effects are already taken into account at NLL. However, the precision of the NNLL calculation, in particular the strong reduction of the scale dependence, still provides a significant theoretical and phenomenological improvement.

In order to assess the improvement in scale dependence in a more detailed way, we show in Fig. 3 results for the predicted cross section as a function of μ/M (where again $\mu_R = \mu_F \equiv \mu$), using a fixed pair invariant mass $M = 5.125$ GeV, which corresponds to the left-most point in Fig. 2. The dot-dashed line corresponds to the variation of the NLL resummed cross section, where for ξ_R in Eq. (49) we include only the first term in the exponent, i.e. $2b_0\alpha_s \ln(\mu_R^2/\hat{m}^2)$. This

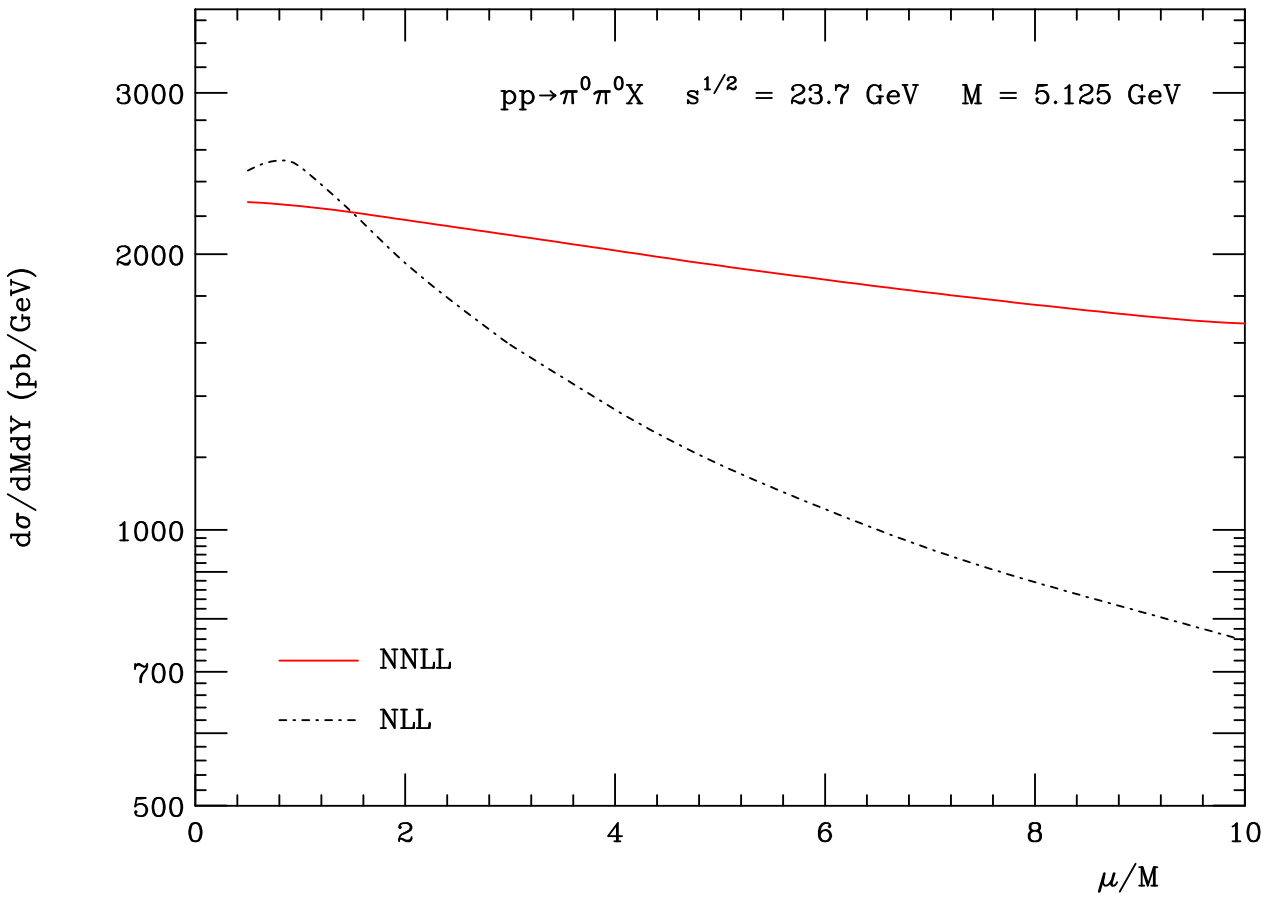

Figure 3: Comparison of the scale dependence of the NLL resummed (dot-dashed) and the NNLL resummed (solid) cross sections for NA24 kinematics. We choose a pion pair invariant mass of $M = 5.125$ GeV and show the variation of the cross sections as a function of μ/M, where $\mu_R = \mu_F = \mu$.

is the only term justified for a cross section resummed to this accuracy. We note that keeping this term in the exponent or expanding the exponential to first order (as done in [16]) makes only a modest numerical difference. At NNLL, we include the full exponent ξ_R in Eq. (49), keeping in mind the discussion following Eq. (51). Our result for the scale variation of the NNLL resummed cross section is shown as a solid line in Fig. 3. One observes a very strong improvement when going from NLL to NNLL, with the NNLL resummed cross section rather flat even out to scales as large as $\mu = 10M$.

Figure 4 shows the comparison of our results to the CCOR data [20]. The main features of the results are very similar to those in Fig. 2. Again the scale dependence is strongly reduced at NNLL. As a side remark we note that the new fragmentation functions of [48] also help to achieve a much better description of the data than we found in our previous study [16].

Finally, we consider di-hadron production in pp collisions at RHIC with a c.m.s. energy of $\sqrt{S} = 200$ GeV. For simplicity, we use the same cuts as for the NA24 experiment. In Fig. 5, we show our results for an invariant mass range of $M = 10 - 75$ GeV. We find that at this energy the full NLO (dashed) and the NLO expansion of the resummed result (crosses) do not match quite as

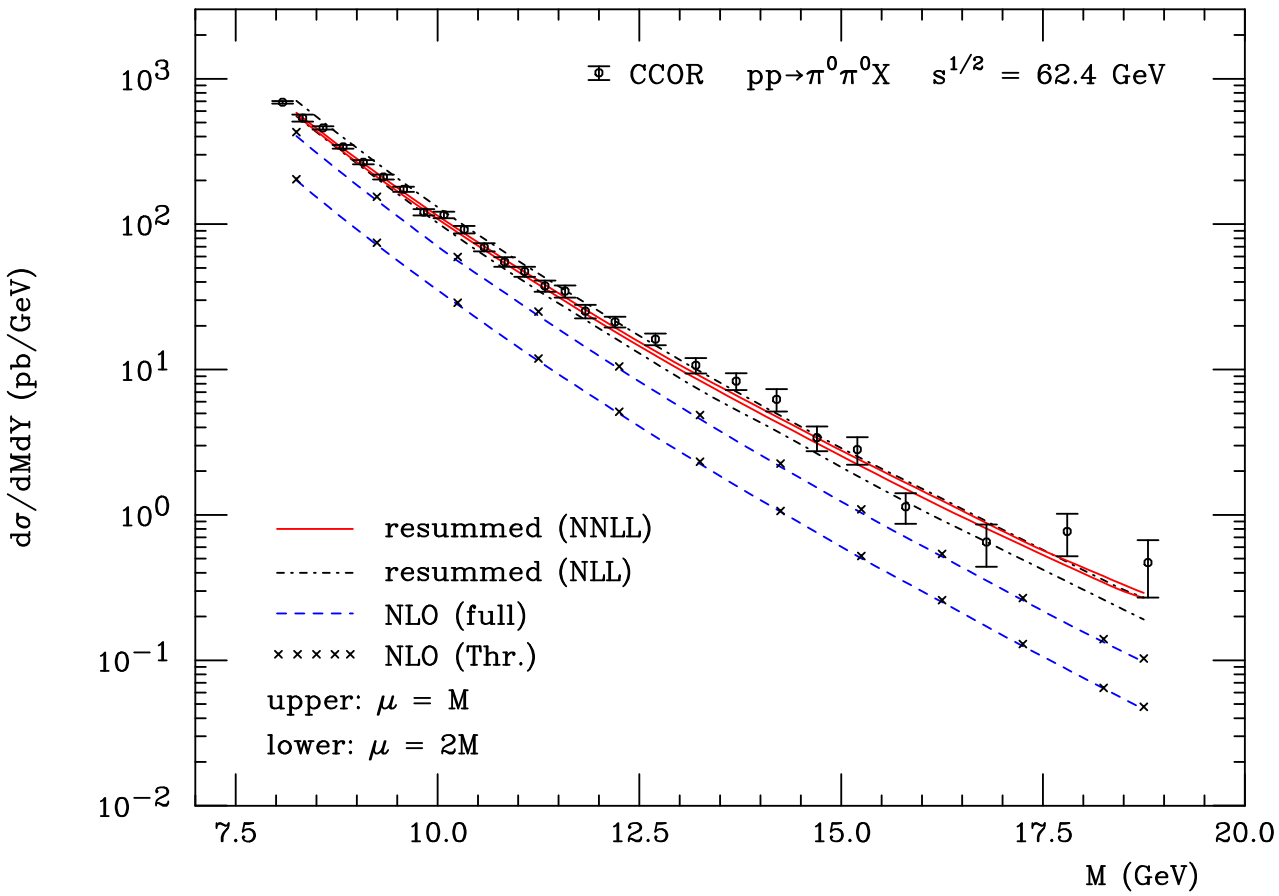

Figure 4: Same as Fig. 2, but for pp-collisions at $\sqrt{S} = 62.4$ GeV. The data are from CCOR [20].

well as observed for fixed target scattering in Fig. 2, although the agreement is usually at the 10% level or better. Threshold resummation again yields a sizable enhancement over NLO, but the effects are somewhat smaller than in the fixed-target regime, since at RHIC's higher energy one is typically further away from threshold. Also here, the NNLL-resummed result is nearly within the NLL scale uncertainty band and shows a reduced scale dependence.

5 Conclusions

We have extended the threshold resummation framework for di-hadron production in hadronic collisions, $H_1H_2 \to h_1h_2X$, beyond the next-to-leading logarithmic level. To achieve this, we have determined the first-order corrections to the hard-scattering function H and the soft function S, which both are matrices in color space. With these, it becomes possible to resum four towers of threshold logarithms in the perturbative series. In our numerical studies, we have found that the NNLL resummed results fall within the scale uncertainty band of the NLL resummed calculation. They also show a much reduced scale dependence.

There are important further applications of our work. Of particular interest are di-jet, single-

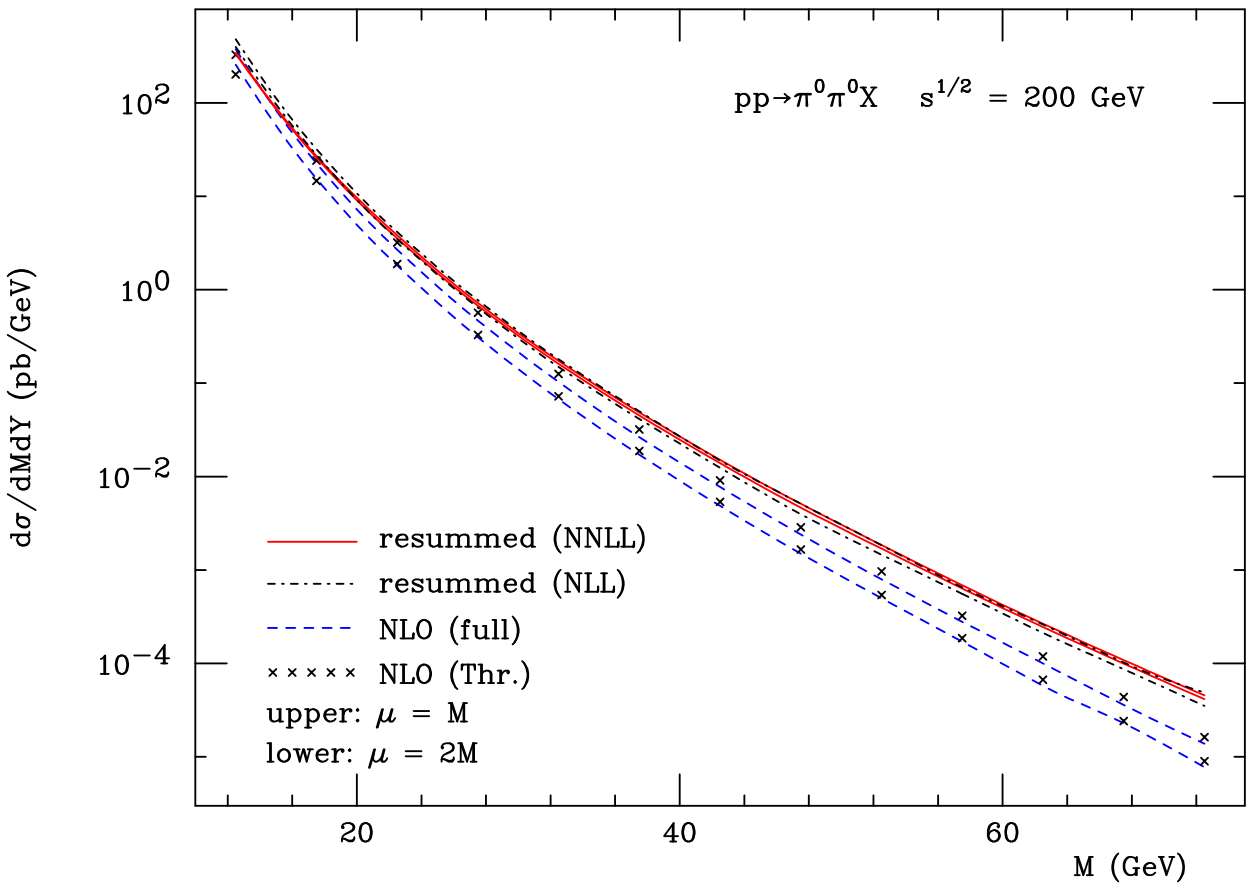

Figure 5: Di-hadron production at RHIC at a center-of-mass energy of $\sqrt{S} = 200$ GeV. The full NLO result (dashed) is shown in comparison to the NLO expansion of the resummed result (crosses). The solid line shows the NNLL resummed cross section. As before, we use the scales $\mu_R = \mu_F = M$ and $\mu_R = \mu_F = 2M$.

inclusive jet and single-inclusive hadron cross sections, all of which have much phenomenological relevance at present-day collider experiments. Given the promising results we have obtained for di-hadron production, we may expect that a similar resummation at NNLL for these reactions would also improve the theoretical QCD prediction.

Acknowledgments

We are grateful to Leandro Almeida, Marco Stratmann, and Ilmo Sung for valuable discussions. This work was supported by the "Bundesministerium für Bildung und Forschung" (BMBF, grant no. 05P12VTCTG). The work of GS was supported in part by the National Science Foundation, grants No. PHY-0969739 and No. PHY-1316617.

A The normalization of the soft function

The soft matrix S_{LI} in the resumed cross section in moment space, Eq. (19), is computed as described in Ref. [9]. Its all-orders form is most conveniently exhibited in moment space, as the ratio of the moments of a fully eikonal cross section $\hat{\sigma}_{LI}^{ab\to cd}$ and four factorized jets, two to absorb the factorizing collinear singularities of the incoming parton lines, and two to absorb the collinear singularities of outgoing lines:

$$\left(S_{ab\to cd}\left(\alpha_s(\hat{m}/\bar{N}),\Delta\eta\right)\right)_{LI} \;=\; \frac{\hat{\sigma}_{LI}^{ab\to cd}\left(\frac{\hat{m}}{N\mu_R},\Delta\eta,\alpha_s(\mu_R),\varepsilon\right)}{\prod_{i=a,b}\tilde{j}_{\rm in}^{(i)}\left(\frac{\hat{m}}{N\mu_R},\alpha_s(\mu_R),\varepsilon\right)\prod_{j=c,d}\tilde{j}_{\rm out}^{(j)}\left(\frac{\hat{m}}{N\mu_R},\alpha_s(\mu_R),\varepsilon\right)}\,. \quad \text{(A.1)}$$

As described in Refs. [2, 9], these "in" and "out" jets, $\tilde{j}_{\rm in}$ and $\tilde{j}_{\rm out}$, respectively are defined to match the collinear singularities and radiation phase space in the partonic threshold limit.

The explicit calculation of $(S_{ab\to cd})_{LI}$ at one loop as given here is equivalent to the procedure described in Sec. 3.3. The functions on the right of (A.1), as defined in detail below, are normalized and expanded according to

$$\begin{aligned}
\hat{\sigma}_{LI}^{ab\to cd}\left(\frac{\hat{m}}{N\mu_R},\Delta\eta,\alpha_s(\mu_R),\varepsilon\right) &= (S^{(0)}_{ab\to cd})_{LI} \;+\; \frac{\alpha_s(\mu_R)}{\pi}\,\hat{\sigma}_{LI}^{ab\to cd\,(1)} \;+\; \mathcal{O}(\alpha_s(\mu_R)^2)\,,\\
\tilde{j}_{\rm in}^{(i)}\left(\frac{\hat{m}}{N\mu_R},\alpha_s(\mu_R),\varepsilon\right) &= 1 \;+\; \frac{\alpha_s(\mu_R)}{\pi}\,\tilde{j}_{\rm in}^{(i,1)} \;+\; \mathcal{O}(\alpha_s(\mu_R)^2)\,,\\
\tilde{j}_{\rm out}^{(j)}\left(\frac{\hat{m}}{N\mu_R},\alpha_s(\mu_R),\varepsilon\right) &= 1 \;+\; \frac{\alpha_s(\mu_R)}{\pi}\,\tilde{j}_{\rm out}^{(j,1)} \;+\; \mathcal{O}(\alpha_s(\mu_R)^2)\,, \qquad \text{(A.2)}
\end{aligned}$$

where $S^{(0)}$ is the tree-level soft matrix, defined as in Eq. (54). The first-order expansion of the soft matrix is thus,

$$\left(S^{(1)}_{ab\to cd}\right)_{LI} = \hat{\sigma}_{LI}^{ab\to cd\,(1)} \;-\; (S^{(0)}_{ab\to cd})_{LI}\left[\sum_{i=a,b}\tilde{j}_{\rm in}^{(i,1)} \;+\; \sum_{j=c,d}\tilde{j}_{\rm out}^{(j,1)}\right]. \quad \text{(A.3)}$$

At any loop order, the collinear singularities of the eikonal cross section $\hat{\sigma}_{LI}$ match those of properly-defined incoming and outgoing jet functions. At one loop, this will result in a finite soft function by simple cancellation in Eq. (A.3), as seen in Sec. 3.3. That is, division by the regularized jet functions plays the role of the collinear factorization of the soft function. It also provides finite, factorizing corrections to the soft function, which depend on the definitions of the jets functions. Here we use jet functions defined directly from the eikonal resummations of Drell-Yan and double inclusive cross sections [12]. The choices, defined below, match collinear singularities of the eikonal cross section, and have the advantage of being Lorentz and gauge invariant. They differ from those made in Refs. [2, 9] by finite terms, but the collinear structure is identical. When restricted to the amplitude level, this is the same formalism that was implemented in Refs. [36, 42].

To make the connection to the calculation of the soft function in this paper explicit, we recall that eikonal diagrams are generated by path-ordered exponentials with constant velocities β, which we represent as

$$\Phi_\beta^{(f)}(\lambda_2,\lambda_1;x) = P\exp\left(-ig\int_{\lambda_1}^{\lambda_2} d\eta\;\beta\cdot A^{(f)}(\eta\beta+x)\right), \quad \text{(A.4)}$$

where superscript f represents the color representation of the parton to which this "Wilson line" corresponds. In terms of these path-ordered exponentials, we define products corresponding to scattering, pair annihilation and pair creation. For the case of $2 \to 2$ scattering, the ends of two incoming and two outgoing Wilson lines are coupled locally by a constant color tensor $\mathcal{C}_I$,

$$\begin{aligned} w_I^{(ab\to cd)}(x)_{\{j\}} &= \sum_{\{i\}} \Phi^{(d)}_{\beta_d}(\infty,0;x)_{j_d,i_d}\ \Phi^{(c)}_{\beta_c}(\infty,0;x)_{j_c,i_c} \\ &\quad \times \left(\mathcal{C}_I^{(ab\to cd)}\right)_{i_d i_c, i_b i_a}\ \Phi^{(a)}_{\beta_a}(0,-\infty;x)_{i_a,j_a}\Phi^{(b)}_{\beta_b}(0,-\infty;x)_{i_b,j_b}\,. \end{aligned} \tag{A.5}$$

For pair annihilation, two lines in conjugate representations that come from the infinite past are joined by a color singlet tensor, that is, a simple Kronecker delta,

$$w_0^{(a\bar{a})}(x)_{\{j\}} = \sum_{\{i\}} (\delta)_{i_a,i_{\bar{a}}}\ \Phi^{(\bar{a})}_{\beta_{\bar{a}}}(0,-\infty;x)_{i_a,j_a}\Phi^{(a)}_{\beta_a}(0,-\infty;x)_{i_{\bar{a}},j_{\bar{a}}}\,, \tag{A.6}$$

and similarly for pair creation, using color-conjugate lines that emerge from a point, and extend into the infinite future,

$$\hat{w}_0^{(a\bar{a})}(x)_{\{j\}} = \sum_{\{i\}} \Phi^{(\bar{a})}_{\beta_{\bar{a}}}(\infty,0;x)_{i_a,j_a}\Phi^{(a)}_{\beta_a}(\infty,0;x)_{i_{\bar{a}},j_{\bar{a}}}\ (\delta)_{i_a,i_{\bar{a}}}\,. \tag{A.7}$$

In terms of these operators, the eikonal cross section is defined by

$$\begin{aligned} \hat{\sigma}_{LI}^{ab\to cd}\left(\frac{\hat{m}}{N\mu_R},\Delta\eta,\alpha_s(\mu_R),\varepsilon\right) &= \int_0^1 d\tau\ \tau^{N-1}\ \int\frac{dy^0}{2\pi}\ e^{i\tau\hat{m}y^0} \\ &\quad \times \mathrm{Tr}_{\{j\}}\ \langle 0|\,\bar{T}\left(w_L^{(ab\to cd)\dagger}\left((y^0,\vec{0})\right)_{\{j\}}\right)\ T\left(w_I^{(ab\to cd)}(0)_{\{j\}}\right)|0\rangle \\ &= \int_0^1 d\tau\ \tau^{N-1}\ \sum_\xi\ \delta(\tau\hat{m}-p_\xi^0) \\ &\quad \times \mathrm{Tr}_{\{j\}}\ \langle 0|\,\bar{T}\left(w_L^{(a\bar{a})\dagger}(0)_{\{j\}}\right)|\xi\rangle\,\langle\xi|T\left(w_I^{(a\bar{a})}(0)_{\{j\}}\right)|0\rangle\,, \end{aligned} \tag{A.8}$$

where T represents time-ordering, $\bar{T}$ anti-time ordering, and p_ξ^0 is the energy of state $|\xi\rangle$. The in jet is defined *in terms of its square* in moment space as

$$\begin{aligned} \left(\tilde{j}_{\rm in}^{(a)}\left(\frac{\hat{m}}{N\mu_R},\alpha_s(\mu_R),\varepsilon\right)\right)^2 &= \int_0^1 d\tau\ \tau^{N-1}\ \sum_\xi\ \delta(\tau\hat{m}-p_\xi^0) \\ &\quad \times \mathrm{Tr}_{\{j\}}\ \langle 0|\,\bar{T}\left(w_0^{(a\bar{a})\dagger}(0)_{\{j\}}\right)|\xi\rangle\,\langle\xi|T\left(w_0^{(a\bar{a})}(0)_{\{j\}}\right)|0\rangle\,. \end{aligned} \tag{A.9}$$

With this choice, $\left(\tilde{j}_{\rm in}^{(a)}\right)^2$ is exactly the eikonal Drell-Yan cross section. It was computed to two loops in Ref. [49]. The out jet is defined by the same integrals but with the pair of incoming Wilson lines of the operator $w_0(x)$ replaced by the outgoing pair in $\hat{w}_0(x)$, corresponding to double

inclusive annihilation [26]:

$$\left(\tilde{j}^{(c)}_{\rm out}\left(\frac{\hat{m}}{N\mu_R},\alpha_s(\mu_R),\varepsilon\right)\right)^2 \;=\; \int_0^1 d\tau\;\tau^{N-1}\;\sum_{\xi}\;\delta(\tau\hat{m}-p_\xi^0)$$
$$\times\;{\rm Tr}_{\{j\}}\,\langle 0|\,\bar{T}\left(\hat{w}_0^{(c\bar{c})\dagger}(0)_{\{j\}}\right)|\xi\rangle\,\langle\xi|T\left(\hat{w}_0^{(c\bar{c})}(0)_{\{j\}}\right)|0\rangle\,. \tag{A.10}$$

It is easy to confirm explicitly in Ref. [49] that the calculation of this quantity depends only on the inner products $\beta_a\cdot\beta_{\bar{a}}$ so that the full two-loop calculation and renormalization of this operator is the same for outgoing as for incoming eikonal jets.

The resummation of logarithms of N in this cross section leads precisely to the functions $\ln\Delta_i^N$ in Eq. (25), which summarize factoring NNLL dependence on the moment variable N, as confirmed recently in Ref. [50]. We note, however, that in the NNLL exponentiation as implemented into the expression for the functions Δ_i^N in Eq. (20), the Drell-Yan soft function is treated as an overall prefactor evaluated at the hard scale $\hat{m}$, rather than at $\hat{m}/N$. Logarithms at NNLL that are associated with this shift are already incorporated into the exponent by use of the relation [50]

$$S(\alpha_s(\hat{m}/N)) \;=\; S(\alpha_s(\hat{m}))\exp\left[-\int_{\hat{m}/N}^{\hat{m}}\frac{d\mu}{\mu}\frac{\partial\ln S(\alpha_s(\mu))}{\partial\mu}\right]. \tag{A.11}$$

To match logarithms associated with these factors consistently we include in our definition of Δ_i^N in Eq. (20) an extra factor of $1-(3\alpha_s/4\pi)A_i^{(1)}\zeta(2)$, to account for our definitions of the in- and out-jet functions in terms of Drell-Yan and double inclusive cross sections. The combined factors for all four jet functions match the π^2 contribution in (87), which in turn arises from the explicit π^2 terms in the integrals $dI_{ij}/d\hat{\tau}$ in (83).

References

[1] G. F. Sterman, Nucl. Phys. B **281**, 310 (1987); S. Catani and L. Trentadue, Nucl. Phys. B **327**, 323 (1989); Nucl. Phys. B **353**, 183 (1991).

[2] N. Kidonakis and G. F. Sterman, Nucl. Phys. B **505**, 321 (1997) [arXiv:hep-ph/9705234].

[3] R. Bonciani, S. Catani, M. L. Mangano and P. Nason, Phys. Lett. B **575**, 268 (2003) [arXiv:hep-ph/0307035].

[4] S. Catani, D. de Florian, M. Grazzini and P. Nason, JHEP **0307**, 028 (2003) [hep-ph/0306211].

[5] V. Ahrens, T. Becher, M. Neubert and L. L. Yang, Eur. Phys. J. C **62**, 333 (2009) [arXiv:0809.4283 [hep-ph]]; Phys. Lett. B **698**, 271 (2011) [arXiv:1008.3162 [hep-ph]].

[6] M. Bonvini and S. Marzani, JHEP **1409**, 007 (2014) [arXiv:1405.3654 [hep-ph]].

[7] S. Catani, L. Cieri, D. de Florian, G. Ferrera and M. Grazzini, Nucl. Phys. B **888**, 75 (2014) [arXiv:1405.4827 [hep-ph]].

[8] C. Anastasiou, C. Duhr, F. Dulat, E. Furlan, T. Gehrmann, F. Herzog and B. Mistlberger, Phys. Lett. B **737**, 325 (2014) [arXiv:1403.4616 [hep-ph]].

[9] N. Kidonakis, G. Oderda and G. F. Sterman, Nucl. Phys. B **525**, 299 (1998) [arXiv:hep-ph/9801268]; Nucl. Phys. B **531**, 365 (1998) [arXiv:hep-ph/9803241].

[10] N. Kidonakis and J. F. Owens, Phys. Rev. D **63**, 054019 (2001) [arXiv:hep-ph/0007268].

[11] S. Catani, M. Grazzini and A. Torre, Nucl. Phys. B **874**, 720 (2013) [arXiv:1305.3870 [hep-ph]].

[12] M. Czakon, A. Mitov and G. F. Sterman, Phys. Rev. D **80**, 074017 (2009) [arXiv:0907.1790 [hep-ph]].

[13] V. Ahrens, A. Ferroglia, M. Neubert, B. D. Pecjak and L. L. Yang, JHEP **1009**, 097 (2010) [arXiv:1003.5827 [hep-ph]]; JHEP **1109**, 070 (2011) [arXiv:1103.0550 [hep-ph]]; L. L. Yang, C. S. Li, J. Gao and J. Wang, arXiv:1409.6959 [hep-ph].

[14] W. Beenakker *et al.*, JHEP **1310**, 120 (2013) [arXiv:1304.6354 [hep-ph]]; W. Beenakker *et al.*, arXiv:1404.3134 [hep-ph].

[15] A. Broggio, A. Ferroglia, B. D. Pecjak and Z. Zhang, arXiv:1409.5294 [hep-ph].

[16] L. G. Almeida, G. F. Sterman and W. Vogelsang, Phys. Rev. D **80**, 074016 (2009) [arXiv:0907.1234 [hep-ph]].

[17] C. De Marzo *et al.* [NA24 Collaboration], Phys. Rev. D **42**, 748 (1990).

[18] H. B. White *et al.* [E711 Collaboration], Phys. Rev. D **48**, 3996 (1993); H. B. White, *A Study of angular dependence in parton-parton scattering from massive hadron pair production*, PhD Thesis, FERMILAB-THESIS-1991-39, FSU-HEP-910722, UMI-92-02321, 1991.

[19] M. Begel [E706 Collaboration], *Production of high mass pairs of direct photons and neutral mesons in a Tevatron fixed target experiment*, PhD Thesis, FERMILAB-THESIS-1999-05, UMI-99-60725, 1999.

[20] A. L. S. Angelis *et al.* [CCOR Collaboration], Nucl. Phys. B **209**, 284 (1982).

[21] Z. Kunszt, A. Signer and Z. Trocsanyi, Nucl. Phys. B **411**, 397 (1994) [hep-ph/9305239].

[22] Z. Bern and D. A. Kosower, Phys. Rev. Lett. **66**, 1669 (1991).

[23] Z. Bern and D. A. Kosower, Nucl. Phys. B **379**, 451 (1992).

[24] R. Kelley and M. D. Schwartz, Phys. Rev. D **83**, 045022 (2011) [arXiv:1008.2759 [hep-ph]].

[25] M. Cacciari and S. Catani, Nucl. Phys. B **617**, 253 (2001) [arXiv:hep-ph/0107138].

[26] G. F. Sterman and W. Vogelsang, Phys. Rev. D **74**, 114002 (2006) [arXiv:hep-ph/0606211].

[27] A. Vogt, Phys. Lett. B **497**, 228 (2001) [hep-ph/0010146]; S. Moch, J. A. M. Vermaseren and A. Vogt, Nucl. Phys. B **726**, 317 (2005) [hep-ph/0506288].

[28] J. Kodaira and L. Trentadue, Phys. Lett. B **112**, 66 (1982); Phys. Lett. B **123**, 335 (1983); S. Catani, E. D'Emilio and L. Trentadue, Phys. Lett. B **211**, 335 (1988).

[29] S. Moch, J. A. M. Vermaseren and A. Vogt, Nucl. Phys. B **688**, 101 (2004) [hep-ph/0403192].

[30] S. Catani, D. de Florian and M. Grazzini, JHEP **0105**, 025 (2001) [arXiv:hep-ph/0102227].

[31] R. V. Harlander and W. B. Kilgore, Phys. Rev. D **64**, 013015 (2001) [arXiv:hep-ph/0102241].

[32] T. O. Eynck, E. Laenen and L. Magnea, [arXiv:hep-ph/0305179]; E. Laenen and L. Magnea, Phys. Lett. B **632**, 270 (2006) [arXiv:hep-ph/0508284].

[33] O. V. Tarasov, A. A. Vladimirov and A. Yu. Zharkov, Phys. Lett. B **93**, 429 (1980).

[34] S. A. Larin and J. A. M. Vermaseren, Phys. Lett. B **303**, 334 (1993) [hep-ph/9302208].

[35] M. Sjodahl, JHEP **0909**, 087 (2009) [arXiv:0906.1121 [hep-ph]].

[36] S. M. Aybat, L. J. Dixon and G. F. Sterman, Phys. Rev. Lett. **97**, 072001 (2006) [arXiv:hep-ph/0606254]; Phys. Rev. D **74**, 074004 (2006) [arXiv:hep-ph/0607309]; *see also:* E. Gardi and L. Magnea, JHEP **0903**, 079 (2009) [arXiv:0901.1091 [hep-ph]]; T. Becher and M. Neubert, JHEP **0906**, 081 (2009) [arXiv:0903.1126 [hep-ph]].

[37] D. de Florian and W. Vogelsang, Phys. Rev. D **71**, 114004 (2005) [arXiv:hep-ph/0501258];

[38] D. de Florian and W. Vogelsang, Phys. Rev. D **76**, 074031 (2007) [arXiv:0704.1677 [hep-ph]]; D. de Florian, P. Hinderer, A. Mukherjee, F. Ringer and W. Vogelsang, Phys. Rev. Lett. **112**, 082001 (2014) [arXiv:1310.7192 [hep-ph]].

[39] E. Laenen, G. F. Sterman and W. Vogelsang, Phys. Rev. D **63**, 114018 (2001) [hep-ph/0010080].

[40] A. Kulesza, G. F. Sterman and W. Vogelsang, Phys. Rev. D **66**, 014011 (2002) [arXiv:hep-ph/0202251].

[41] N. E. W. Glover, Nucl. Phys. Proc. Suppl. **116**, 3 (2003) [hep-ph/0211412].

[42] G. F. Sterman and M. E. Tejeda-Yeomans, Phys. Lett. B **552**, 48 (2003) [hep-ph/0210130].

[43] S. Catani, Phys. Lett. B **427**, 161 (1998) [hep-ph/9802439].

[44] W. L. van Neerven, Nucl. Phys. B **268**, 453 (1986).

[45] S. Catani, M. L. Mangano, P. Nason and L. Trentadue, Nucl. Phys. B **478**, 273 (1996) [arXiv:hep-ph/9604351].

[46] J. F. Owens, Phys. Rev. D **65**, 034011 (2002) [arXiv:hep-ph/0110036].

[47] W. K. Tung, H. L. Lai, A. Belyaev, J. Pumplin, D. Stump and C. P. Yuan, JHEP **0702**, 053 (2007) [arXiv:hep-ph/0611254].

[48] D. de Florian, R. Sassot, M. Epele, R. J. Hernandez-Pinto and M. Stratmann, arXiv:1410.6027 [hep-ph].

[49] A. V. Belitsky, Phys. Lett. B **442**, 307 (1998) [hep-ph/9808389].

[50] G. F. Sterman and M. Zeng, JHEP **1405**, 132 (2014) [arXiv:1312.5397 [hep-ph]].